Soil and crop responses to basalt, tephrite and lime amendments in a 16-month maize field trial

Lucilla Boito[1], Teneille Nel[1], Charline Vandenhove[1], Lowie Van Ryckeghem[2], Laura Steinwidder[1], Arthur Vienne[1], Ivan Janssens[2], Sara Vicca[1]

[1]Biobased Sustainability Engineering (SUSTAIN), Department of Bioscience Engineering, University of Antwerp, Antwerp, 2020, Belgium

[2]Plants and Ecosystems (PLECO), Department of Biology, University of Antwerp, Wilrijk, 2610, Belgium

Keywords: enhanced weathering, soil fertility, soil water content, crop responses

Abstract

Enhanced weathering (EW) of silicate minerals has been proposed as a carbon dioxide removal (CDR) strategy with potential co-benefits for soil health and crop productivity. Among the proposed feedstocks, basalt is considered a good candidate feedstock due to its lower heavy metal content compared to olivine-rich rocks such as dunite. However, basaltic feedstocks differ substantially in mineralogical composition, and the implications of this variability for EW co-benefits remain poorly understood, particularly in relatively fertile agricultural soils. In this field experiment, we applied two basalt (Bolsdorfer and Hühnerberg) and a tephrite (Eifelgold) amendment (all at 50 ton ha^{-1}), which differed in mineralogical composition, as well as lime (applied at 2 ton ha^{-1}), to a Belgian maize field (Gleyic Podzol with loamy-sand texture; topsoil pH = 6.66 ± 0.03; cation exchange capacity (CEC) = 7.6 ± 0.13 $cmol^{+}$ kg^{-1}). We assessed the feedstocks' potential to affect topsoil (0-10 cm) volumetric water content (VWC), chemical fertility and crop performance over 16 months.

Hühnerberg, Bolsdorfer and lime increased pore water alkalinity (+87.9%, +65.1%, +51.6% respectively) and DIC (+111.0%, +97.2%, 74.4% respectively), indicating active weathering. Other treatment effects were modest and mostly short-lived. Bolsdorfer, Hühnerberg and lime significantly increased soil pH (+0.52 ± 0.06, + 0.53 ± 0.09, +0.37 ± 0.08 respectively; mean ± SE) and base saturation (+21.1% ± 4.0, +18.8% ± 6.0, +20.8% ± 6.8 respectively; mean ± SE) after the first growing season, but these early responses dissipated over time. None of the treatments significantly affected CEC, while effects on VWC were growing season- and treatment-specific. Crop biomass and quality, including plant Ni and Cr content, were unaffected, aside from minor shifts in nutrient concentrations. Overall, EW co-benefits for soil water content, soil chemical fertility and crop biomass were limited and dependent on amendment mineralogy. The observed short-term improvements in soil chemical fertility did not translate into greater crop biomass, suggesting that the agronomic benefits of basalt amendments may be limited in relatively fertile, near-neutral soils. Importantly, the absence of adverse effects on crop biomass and quality suggests that silicate rock application did not compromise crop performance under the conditions investigated.

Introduction

Climate change is widely recognized as one of the most pressing global challenges. It contributes to social disruption, biodiversity loss, and economic instability, with these impacts expected to intensify as climate-related disasters become more frequent and severe (Garcia-Leon et al., 2021; Habibullah et al., 2022). Addressing these consequences requires not only steep emissions reductions, but also the deployment of carbon dioxide removal (CDR) technologies (Ipcc, 2022). One promising approach is enhanced weathering (EW) of silicate minerals, which builds on the natural geochemical process in which silicate minerals react with carbon dioxide (CO_2) and water to form dissolved (bi)carbonate ions. These (bi)carbonate ions can either be transported out of the system through groundwater and riverine fluxes, or precipitate as pedogenic carbonates within the soil (Beerling et al., 2020; Beerling et al., 2018; Fuss et al., 2018). EW accelerates this process by grinding silicate rocks into fine powders, thereby increasing their reactive surface area (Hartmann et al., 2013; Schuiling and Krijgsman, 2006). In particular, applying silicates to agricultural soils offers a practical advantage over land-intensive CDR methods such as afforestation and reforestation, as it utilizes existing farmland without competing for land use (Beerling et al., 2018).

EW has the potential to deliver multiple co-benefits for soil health and crop productivity. One of the most significant is its potential to improve soil chemical fertility by increasing soil pH and cation exchange capacity (CEC), both of which influence nutrient availability and retention (Anda et al., 2015; Conceição et al., 2022; Gillman, 1980). Soil pH plays a central role in regulating the mobility of elements: at low pH values, essential nutrients become less available to plants, while harmful trace metals such as nickel (Ni) and zinc (Zn) are increasingly mobilized (Kabata-Pendias, 2000; Loomis and Morris, 1983). Upon weathering, silicates can also generate metal (hydr)oxides and secondary clay minerals, thereby increasing the clay-sized fraction of the soil and, in turn, its CEC (Righi and Meunier, 1995). Accordingly, EW has been shown to promote plant growth and crop yield, especially in acidic or nutrient-depleted soils (Goll et al., 2021; Shamshuddin et al., 2011; Vaghetti Luchese et al., 2021), while responses in more fertile agricultural soils have generally been more limited (Swoboda et al., 2022). Silicate dissolution also supports gradual nutrient release, including magnesium (Mg), calcium (Ca), potassium (K) and phosphorus (P), which are essential for plant growth and can enhance crop yield and quality (Beerling et al., 2018).

On the other hand, EW may also entail undesirable environmental effects. One potential concern is a reduction in soil hydraulic conductivity following feedstock application, which may result from the partial occlusion of soil pores by fine (silty to clayey) amendment particles (Akortey et al., 2026; Amann and Hartmann, 2019; Levy et al., 2024). Such blockages could reduce water infiltration and alter water flow pathways (Akortey et al., 2026; Amann and Hartmann, 2019; Hillel, 1998). Especially in systems where silicate materials are applied to the soil surface with little to no incorporation, reduced infiltration may increase surface runoff and limit water movement into deeper soil layers (Amann and Hartmann, 2019; Clarkson et al., 2024), potentially decreasing soil water availability within the rooting zone. Conversely, when silicate feedstocks are well-incorporated into the plough layer, they may increase soil water retention and plant-available water (Akortey et al., 2026; De Oliveira Garcia et al., 2020). Under water-limited conditions, such effects could improve crop drought resilience. The agronomic implications for water availability are likely to be context-dependent, depending on the impact of EW on soil texture and structure, as well as interactions with climatic conditions, crop characteristics, biological activity (e.g.,

82 earthworm-mediated macropore formation), and management practices such as feedstock
83 application rate and degree of soil incorporation.

84 Another potential risk associated with EW is the accumulation of heavy metals introduced
85 through the applied rock material (Suhrhoff, 2022; Hartmann et al., 2013; Renforth, 2012).
86 Elevated soil pH induced by silicate weathering generally decreases the mobility of trace metals
87 like nickel (Ni) and zinc (Zn), thereby promoting their retention in the soil and reducing their
88 immediate bioavailability (Basta et al., 1993). However, this immobilization does not eliminate
89 the environmental risks associated with EW: should soil acidification occur in the future, for
90 example as a result of land-use change, management intervention, or natural pedogenic
91 processes, previously retained metals may become mobilized. The subsequent release of heavy
92 metals could increase their transport to groundwater and/or their uptake by crops. Consequently,
93 the long-term environmental safety of EW requires careful consideration (Hartmann et al., 2013).

94 Basalt is one of the most commonly used silicate rocks in EW applications due to its long history
95 of agricultural use, widespread availability, and generally low concentrations of the toxic
96 elements Ni and chromium (Cr) (Dupla et al., 2023; Gislason and Oelkers, 2014; Skov et al., 2024;
97 Swoboda et al., 2022; Van Straaten, 2002). However, the mineralogical and elemental
98 composition of basalt often varies. This heterogeneity can influence weathering rates and
99 therefore the nature of its co-benefits and risks (Gudbrandsson et al., 2011; Palandri and Kharaka,
100 2004; Te Pas et al., 2023), with heavy metal content spanning from safe to potentially concerning
101 levels (Dupla et al., 2023). For instance, while basalts rich in olivine weather more rapidly, they
102 may release higher concentrations of heavy metals such as Ni and Cr (Beerling et al., 2018),
103 thereby posing potential trade-offs between CDR efficacy and environmental safety.

104 Despite growing interest in EW and increasing efforts to compare CDR potential and associated
105 co-benefits of different feedstocks (Rijnders, 2025; Steinwidder et al., 2025; Te Pas et al., 2023),
106 field-based comparisons among basalts and tephrites with contrasting mineralogical
107 compositions remain scarce. Similarly, relatively few studies have evaluated silicate
108 amendments alongside conventional practices such as agricultural liming (Araujo et al., 2024;
109 Buckingham and Henderson, 2024; Dietzen et al., 2018). Moreover, evidence for EW-induced
110 agronomic benefits derives primarily from acidic, highly weathered, or nutrient-limited soils,
111 whereas relatively fertile agricultural soils, which are likely targets for EW deployment focused on
112 CDR rather than agronomic improvement, have received less attention and generally show
113 weaker responses (Swoboda et al., 2022; Van Straaten, 2002). Consequently, it remains unclear
114 whether mineralogical differences among basaltic feedstocks lead to contrasting effects on soil
115 water dynamics, chemical fertility and crop productivity under field conditions.

116 To address these knowledge gaps, we conducted a field experiment with maize (*Zea mays* L.,
117 1753) to assess the effects of two basalt types, one tephrite, and agricultural lime on soil VWC,
118 chemical fertility, and crop performance. By comparing amendments with distinct mineralogical
119 profiles under the same field conditions, we aimed to determine whether feedstock mineralogy
120 gives rise to contrasting agronomic benefits or risks. We hypothesized that silicate and lime
121 amendments would i) increase soil VWC, owing to a decrease in hydraulic conductivity resulting
122 in increased water retention, ii) improve soil chemical fertility indicators, specifically soil pH, CEC
123 and base saturation, and finally iii) positively affect crop yield and quality, without an increase in

heavy metal content. Overall, we anticipated stronger effects from faster-weathering silicates, which more rapidly release cations, increase soil pH and contribute to the formation of oxides and clays, which ultimately increase CEC. Finally, we hypothesized that lime would produce more immediate but shorter-lived effects compared to silicates, owing to its faster dissolution rate.

Materials and methods

A field experiment was setup in an agricultural field and located in Westmalle, Belgium (51°17'50.3"N, 4°39'54.6"E). The regional climate is temperate maritime with mild winters and warm summers, and the location experiences an average precipitation of 850 mm $year^{-1}$, and a mean annual temperature of 11 °C (Koninklijk Meteorologisch Instituut Van België, 2026; Kottek et al., 2006). The soil at the experimental site is classified as a loamy sand (sand: 79.58%, silt: 19.18 %, clay: 1.24%) Gleyic Podzol (World Reference Base; Dondeyne et al., 2014). Key soil properties include a near-neutral pH of 6.66 ± 0.03, a relatively high SOC content of 2.7% ± 0.15 and CEC of 7.6 ± 0.13 $cmol^{+}$ kg^{-1}. Bulk density varied depending on the timing of measurement, particularly because of ploughing (Figure S1). The site belongs to the Mintjens Group NV and covers an area of approximately 4.9 ha. The field is typically used to cultivate crops for cattle feed such as maize, triticale, or ryegrass, and during the winter season, a cover crop (either triticale or mustard) is often grown. The experimental site is fertilized annually using both manure (170 kg nitrogen (N) ha^{-1}) and calcium ammonium nitrate (150 kg ha^{-1}; nitrate (NO_3^-) = 13.5%; ammonium (NH_4^+) = 13.5%; calcium (Ca) = 6%), and all agricultural operations (i.e., fertilizing, ploughing, sowing, herbicidal application, harvesting) are performed using machinery. Maize is generally planted between April and June, depending on weather conditions, and harvested between September and November.

To evaluate the effects of different silicate types, as well as lime, on soil and crop parameters, five treatments (Table 1) were randomly established in 10 × 10 m plots: two basalt types (Bolsdorfer, mined at 50°16'34.4"N 6°40'28.7"E; Hühnerberg, mined at 50°42'28.1"N 7°20'13.2"E) and a tephrite (Eifelgold, mined at 50°26'23.7"N 7°16'44.7"E) were provided by Rheinische Provinzial-Basalt- und Lavawerke (RPBL). These silicates differed in their mineralogical composition but had similar particle size distribution (d80 = 62.3, 84.4 and 78.4 µm for Hühnerberg, Eifelgold and Bolsdorfer respectively; Table 2-3; Figure S2-S4). In addition, one lime ($CaCO_3$; AVEVE) treatment and an unamended control were also established. Each treatment was replicated three times, resulting in a total of 15 plots. Amendments were applied once, on 22-23-24 May 2023, after ploughing but prior to maize (*Zea mays* L., 1753) sowing. Silicate amendments were applied at 50 t ha^{-1}, a common application rate in EW experiments (Steinwidder et al., 2025; Suhrhoff et al.,

***Table 1**: Overview of the experimental design. For each treatment, the associated feedstock type and application amount are specified.*

Treatment name	Feedstock added	Amount (t ha^{-1})
Control	None	-
Lime_02	Limestone (Calcium carbonate)	2
Bolsdorfer_50	Bolsdorfer (Basalt)	50
Eifelgold_50	Eifelgold (Tephrite)	50
Huhnerberg_50	Hühnerberg (Basalt)	50

2024), while lime was applied at a lower rate of 2 t ha^{-1} to reflect realistic agricultural practices. Amendments were manually distributed on the soil surface without incorporation into the soil; however, farming machinery was deployed in the field following amendment to sow the maize (on 26 May 2023), leading to feedstock incorporation into the soil. The data collection period spanned two consecutive growing seasons and the fallow period between them (539 days; first growing season = 26 May to 11 October 2023; second growing season = 19 June to 12 November 2024). During the fallow period, maize plants (remaining after harvesting of the cobs) were retained, and no cover crop was sown. To minimize edge effects, all sampling was conducted within the central 5 × 5 m core of each plot. Soil VWC was monitored using a TMS soil moisture sensor (TMS, TOMST) installed in the centre of each plot. Sensors were inserted vertically into the soil to record data within the 0-10 cm layer. Measurements were recorded at 15-minute intervals throughout the experimental period. VWC sensors were temporarily removed between day 25 (15 June 2023) and day 30 (20 June 2023) to allow access to the field for agricultural machinery.

Pore water sampling

Pore water was sampled once before amendment (25 April 2023), three times during each growing season, and two times during the fallow period between them, using rhizon samplers (Macrorhizon, 19.21.35; Rhizosphere Research Products B.V.) installed vertically in the soil at a

***Table 2**: Mineralogy of the applied basalts expressed in wt % obtained by XRD analysis. XRD patterns were recorded using a Panalytical X'Pert PRO MPD Θ-Θ diffractometer (Cu-Kα radiation generated at 40 kV and 40 mA), equipped with a variable divergence slit (20 mm irradiated length), primary and secondary soller, Scientific ẌCelerator detector (active length 0.59°), and a sample changer (sample diameter 28 mm).*

Mineral	**Mineral formula**	**Bolsdorfer**	**Eifelgold**	**Hühnerberg**
SILICATES				
Nepheline	$(Na,K)AlSiO_4$	31	10.5	
Plagioclase	$(Na,Ca)(Si,Al)_4O_8$		14.5	26.5
K-Feldspar	$KAlSi_3O_8$		1.5	5
Muscovite	$KAl_2(AlSi_3O_{10})(F,OH)_2$	3	6.5	3
2:1 layer silicates	$(K,H_3O)(Al,Mg,Fe)_2(Si,Al)_4O_{10}[(OH)_2,H_2O]$			27.5
Kaolinite	$Al_2Si_2O_5(OH)_4$			1.5
Leucite	$KAlSi_2O_6$		12	
Analcime	$NaAlSi_2O_6•(H_2O)$			1
Diopside	$MgCaSi_2O_6$	45	41.5	23
Forsterite	Mg_2SiO_4	4	5	6.5
Åkermanite	$Ca_2Mg[Si_2O_7]$	6.5		
PHOSPHATES				
Fluorapatite	$Ca_5(PO_4)_3(OH,F,Cl)$	4.5	2.5	1
SULPHATES				
Pyrite	FeS_2			0.5
OXIDE/HYDROXYDES				
Magnetite	$Fe^{2+}Fe_2^{3+}O_4$	7.5		5.5
Hematite	Fe_2O_3		6	

depth of 0-10 cm and connected to 50-ml luer-lock syringes (Fisher Scientific BV) to generate suction. Prior to sampling, 710 ml of rainwater collected in underground storage tanks at the University of Antwerp was gently applied to the soil surrounding each rhizon sampler and allowed to infiltrate completely. Subsequentially, a vacuum was created in the syringe, and pore water was collected for analysis.

Pore water analyses included alkalinity, pH and concentrations of dissolved inorganic carbon (DIC), and the metals Al, Na and Ni. Soil pore water pH was measured with a flat membrane electrode (6.0256.100; Metrohm) connected to a 914 pH/Conductometer (2.914.0020, Metrohm). DIC was measured on three technical replicates with a TOC analyser (FormacsTM HT Series, Skalar); whereas alkalinity was measured on three technical replicates by a continuous flow analyser (SAN++® Advanced Series, Skalar). Elemental analyses (Al, Na, Ni) were performed on samples acidified with 1.5 ml 70% nitric acid (HNO_3) by inductively coupled plasma-optical emission spectrometry (ICP-OES; iCAP6300 Duo; Thermo Fisher Scientific). DIC and elemental analyses were conducted in-house on samples filtered through a disposable 0.45 µm PET-45/25 membrane filter (CHROMAFIL, Macherey-Nagel). Alkalinity and pH measurements were carried out on unfiltered samples.

***Table 3**: Elemental composition of the applied silicates. Bulk-rock geochemical analysis was determined by X-ray fluorescence spectrometry at the Geochemistry laboratory of the Federal Institute for Geosciences and Natural Resources, Hannover, Germany. The major and minor element composition was determined with a PANalytical Zetium wavelength dispersive XRF spectrometer on melt beads from samples powdered by using an agate ring mill. The samples were then further prepared by mixing with a flux material (lithium metaborate Spectroflux, Flux No. 100A, Alfa Aesar) and then heated to form molten glass beads.*

Element	Unit	Eifelgold	Bolsdorfer	Hühnerberg	Element	Unit	Eifelgold	Bolsdorfer	Hühnerberg
Si	wt %	43.1	38.9	42.9	Cu	ppm	60	102	55
Ti	wt %	2.8	2.6	1.9	Ga	ppm	17	17	15
Al	wt %	14.2	11.7	11	Hf	ppm	<22	<22	<21
Fe	wt %	11.3	11.1	11.6	La	ppm	61	99	62
Mn	wt %	0.2	0.2	0.2	Mo	ppm	<8	<8	<8
Mg	wt %	8.6	9.5	13.4	Nb	ppm	77	138	62
Ca	wt %	11.5	16.3	9.1	Nd	ppm	53	99	51
Na	wt %	3.1	3.5	1.8	Ni	ppm	100	118	382
K	wt %	3.3	2.4	1	Pb	ppm	<8	<8	<8
P	wt %	0.6	1.1	0.6	Rb	ppm	73	60	31.5
S	wt %	0.1	0.3	0.1	Sb	ppm	<17	<17	<17
Cl	wt %	0.03	0.04	0.01	Sc	ppm	32	32	<28
F	wt %	0.1	0.2	0.1	Sm	ppm	<26	<26	<26
LOI	wt %	0.7	1.7	6	Sn	ppm	<21	<21	<21
As	ppm	<4	<4	<3	Sr	ppm	834	1418	659
Ba	ppm	1020	1119	494	Ta	ppm	<15	<15	<15
Bi	ppm	<7	<7	<7	Th	ppm	10	18	8
Ce	ppm	121	209	93	U	ppm	<7	<7	<7
Co	ppm	43	38	56	V	ppm	296	384	191
Cr	ppm	150	251	408	W	ppm	<13	<13	<13
Cs	ppm	<60	<63	<57					

Soil sampling and analyses

Topsoil (0-10 cm) samples were collected in triplicate from each plot before amendment (on 19 April 2023), during the fallow period (on 13 February 2024), at the start of the second growing season (on 23 July 2024) and at the end of each growing season (on 04 October 2023 and 23 September 2024), and subsequently air-dried. Soil pH was measured individually for each of the triplicate samples by suspending 4 g of air-dried soil in 10 mL of deionized water (soil : water = 1 : 2.5). The suspensions were shaken by hand for 30 s, allowed to settle for one hour, and then briefly shaken before measuring their pH. Soil potential CEC and base saturation were determined by 1 M ammonium acetate (NH_4OAc) displacement at pH 7.0 using ICP-OES (iCAP6300 Duo; Thermo Fisher Scientific; Brown, 1943) after pooling together the three soil sample replicates from each plot.

Biomass sampling and analysis

At the end of each growing season (on 04 October 2023 and 23 September 2024) above- and below-ground plant biomass was sampled. In each plot, a fixed area of 0.36 m^2 was randomly selected, ensuring the inclusion of maize plants from three different corn rows (Figure S5). All plants within the sampling area were cut as close to the soil surface as possible and then removed. In the laboratory, the top three leaves of each plant were sampled, whereafter the aboveground biomass was further separated into stems (which included tassels), remaining leaves and corn. The fresh weight of each component was then recorded, before drying the plant material at 70 °C for 48 hours or until a constant weight was achieved, after which the dry biomass was determined.

To assess belowground biomass, root samples were collected from within the same 0.36 m^2 area defined for above-ground biomass sampling, using a 100 cm^3 Kopecky ring to extract soil and roots from the middle of the 0-10 cm layer. In each plot, three samples were taken adjacent to a cut plant ("plant root" samples), and two samples were taken from the centre of the corn row ("midrow" samples). Once in the laboratory, root samples were cleaned by gently rinsing them with tap water over a 1 mm mesh sieve and picking root materials out by hand. All belowground biomass samples were then dried at 70 °C for 48 hours, and their dry weight was recorded. In order to estimate the total belowground biomass in each plot from the "plant root" and "midrow" samples, we first determined the proportion of the sampled plot area represented by each sample type. We assumed "plant root" samples to be representative of a circular area with a radius of approximately 10 cm around each maize plant, while "midrow" samples represented the remaining area between corn rows. To quantify these proportions, we analysed three randomly selected pictures of the 0.36 m^2 sampling area taken during the harvest from three different plots using ArcMap (Esri, 2011). On average, the area associated with "plant root" samples accounted for 16% of the total sampled area, whereas "midrow" samples represented the remaining 84%. These percentages were then used to scale root biomass estimates to the plot level.

Plant samples were analysed for nutrients and heavy metals as follows. Before analysis, the three top leaves (hereafter referred to as leaves), stems, corn kernels and roots were ground using an ultra-centrifugal mill (ZM 200, Retsch GmbH) with a 0.25 mm mesh size sieve. To quantify Ca, Cr, Fe, K, Mg, Na, Ni, P, and Zn contents, a 0.2 g sample of dried and homogenized plant material was subjected to acid digestion with 70% HNO_3 at 60 °C for 30 minutes, followed by the addition of 30% hydrogen peroxide (H_2O_2) and further heating at 120 °C for 90 minutes. After cooling and filtering, elemental concentrations were measured by ICP-OES (Thermo Scientific, iCAP 6300

Duo). Biogenic Si was determined by digestion of a 0.03 g plant sample with 25 ml 0.5 M sodium hydroxide (NaOH) and then analysed with a continuous flow analyser (SAN++® Advanced Series, Skalar) following Demaster (1981) and Saccone et al. (2007). Between 4 and 8 mg of plant material was used to perform elemental C and N analyses by Dumas dry combustion method using a Flash 2000 CN Soil Analyzer (Interscience, Louvain-la-Neuve, Belgium).

Data analysis

All statistical analyses were performed in R using packages nlme, lmertest, dunn.test and emmeans (Dinno, 2024; Lenth, 2026; Kuznetsova et al., 2017; Pinheiro et al., 2007; R Core Team, 2024). The level of significance for all analyses was set at $p < 0.05$. Interactions terms were tested and excluded from the final models if statistically insignificant. Data collected prior to field amendment was excluded from statistical analyses but is shown in the figures with reduced opacity for visual reference.

To assess the effects of treatment and time on maize biomass density and quality, a factorial analysis of variance (ANOVA) was performed, with treatment and growing season as fixed effects and plot as a random effect. If normality or homoscedasticity of the model residuals were not met after log- or square-root transformation, the non-parametric Kruskal-Wallis test was used with treatment as explanatory variable. A post-hoc test (Tukey's honestly significant difference test or Dunn's multiple comparison test for parametric and non-parametric analyses respectively) was conducted to explore significant differences among treatments. While full ANOVA results are presented in the supplementary information (Table S6), only significant findings are reported and discussed in the main text.

To investigate treatment effects on pore water characteristics (pH, DIC, alkalinity, Al, Na, Ni), VWC, soil pH, CEC, and base saturation, a linear mixed model was constructed with plot as random effect, days as continuous covariate and treatment as class covariate (Table S7). VWC data was obtained from sensor data following Kopecky et al. (2021). Post-hoc comparisons of linear mixed models were performed using estimated marginal means. For models including a treatment x day interaction, treatment-specific slopes were estimated using the emtrends() function and compared pairwise using Tukey-adjusted tests.

Ni concentrations in all corn samples collected in 2023 and 2024 were below the limit of quantification (LOQ; 0.0002 mg g^{-1}); consequently, corn Ni data were excluded from further analyses. Although Ni concentrations were also below the LOQ in most stem and leaf samples in 2024 and in all pore water samples collected between 25 July and 25 October 2023, these values were retained and set to zero for subsequent analyses.

The data and model code in support of our findings are openly available in Zenodo at https://doi.org/10.5281/zenodo.23803780 (Boito, 2026).

Results

Weathering signals: pore water pH, DIC and alkalinity

Pore water DIC and alkalinity significantly decreased over time, and significant treatment effects were observed on pore water pH, DIC and alkalinity. Specifically, Hühnerberg basalt significantly increased pore water pH (+0.36 ± 0.06), DIC (+5.02 ± 0.95 mg l^{-1}) and alkalinity (+0.46 ± 0.1) compared to control (all values are means ± SE; Figure 1; Table S7). Similarly, Bolsdorfer basalt significantly increased alkalinity (+0.34 ± 0.1 meq l^{-1}) and DIC (+4.41 ±1.33 mg l^{-1}) compared to control, while lime significantly increased DIC compared to control (+3.38 ± 0.86 mg l^{-1}).

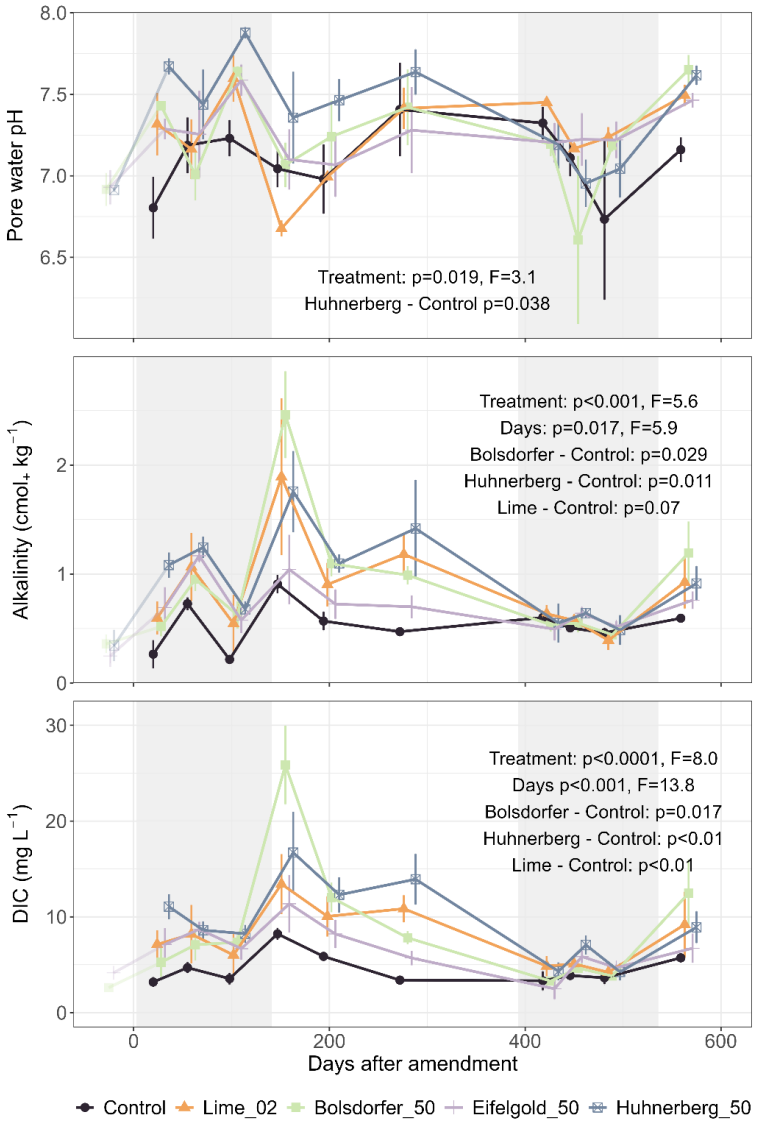


***Figure 1**: Average pore water pH (top), alkalinity (middle) and DIC (bottom) concentrations throughout the experiment for each treatment. Error bars represent the standard error on the mean. Shadowed areas represent the growing seasons. Significant p- and F-values are shown from a linear mixed model with pore water pH, alkalinity or DIC as response variable, days as continuous covariate, treatment as class covariate and plot as random effect. Significant pairwise comparisons from post-hoc tests are shown. Significant interaction effects, when present, are indicated in the plot by an "x". When interactions were not significant, they were excluded from the model and not shown here. See Table S7 for complete statistics.*

Effects on VWC, soil fertility and nutrient availability

A treatment effect on VWC emerged during the first growing season, although the response was limited to specific amendments (Figure 2; Table S7). Relative to control, VWC increased significantly faster over time in the Eifelgold (2.04-fold) and Hühnerberg treatments (1.87-fold; significant treatment x day interactions). In contrast, no significant effects were observed for Bolsdorfer or lime during this period. Interestingly, this pattern changed during the fallow period, with treatment effects reversing direction: rather than promoting higher VWC, Hühnerberg and lime both accelerated its decline over time 1.76-fold compared to control. Bolsdorfer also showed a significantly steeper decline compared to control (1.59-fold relative to the control). However, visual inspection of the time series showed that the Bolsdorfer response should be interpreted with caution. Throughout most of the fallow period, Bolsdorfer VWC remained similar to that of the control treatment, and the significant effect was largely driven by a decrease in VWC after day 284. Thus, the Bolsdorfer-amended treatment appeared to diverge from the control only

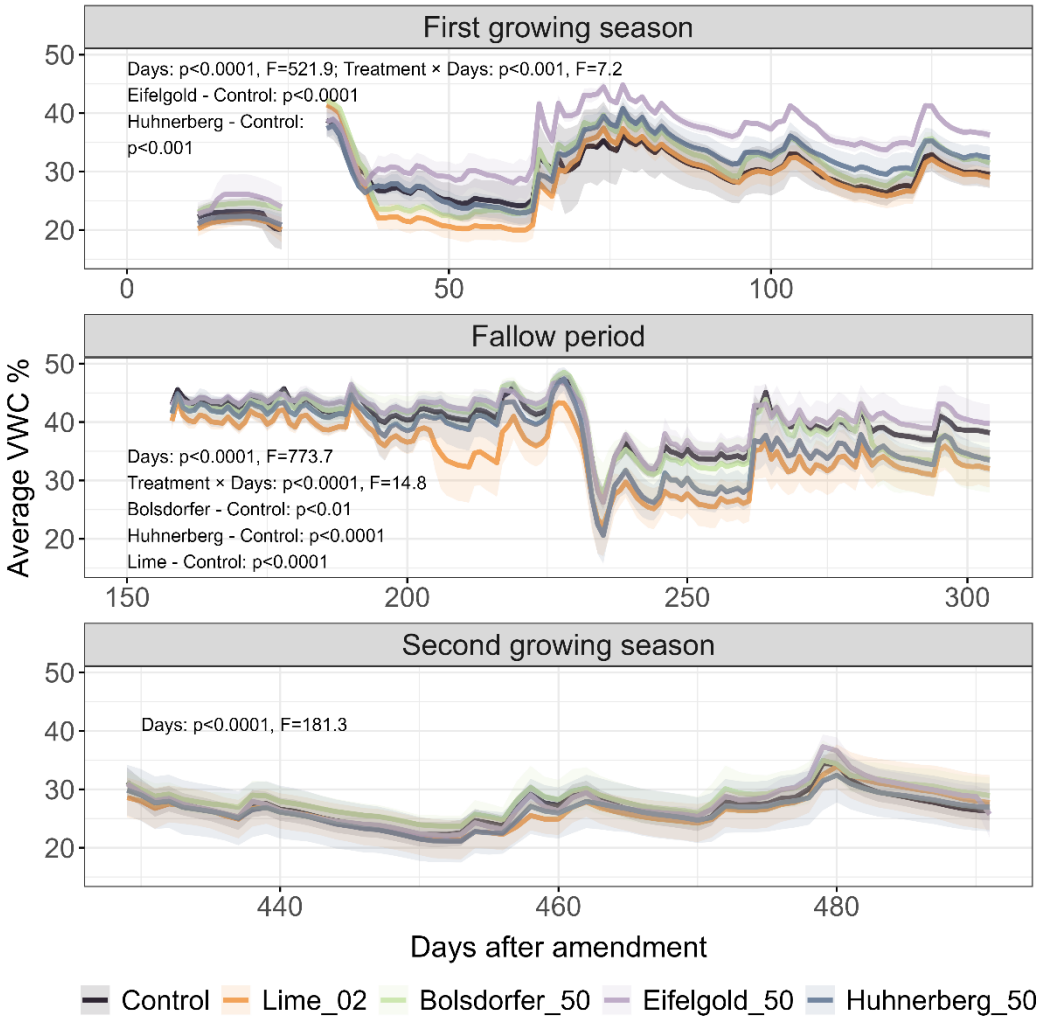


Figure 2: *Average daily VWC for each treatment (n = 3) over the first growing season (top), the fallow period (middle) and the second growing season (bottom). Shaded areas represent standard errors on the mean. Significant p- and F-values are shown from a linear mixed model with VWC as response variable, days as continuous covariate, treatment as class covariate and plot as random effect. Significant interaction effects, when present, are indicated in the plot by an "x". Significant pairwise comparisons are shown. When interactions were not significant, they were excluded from the model and not shown here. See Table S7 for complete statistics.*

towards the end of the fallow period. Finally, no treatment effects were detected during the second growing season.

In general, soil pH significantly declined over time (Figure 3). Interestingly, at the first sampling after amendment (day 135), a significant treatment effect was observed: Bolsdorfer (+0.52 ± 0.06), Hühnerberg (0.52 ± 0.09) and lime (0.37 ± 0.08) significantly increased soil pH compared to control (values are means ± SE; Table S7). However, this effect was temporary and disappeared later, as indicated by a significant treatment x days interaction effect. CEC increased over time and was not significantly affected by treatment, despite a non-significant increase in CEC at day 135 with Bolsdorfer, Hühnerberg and lime (Figure 3; Table S7). Similarly to soil pH, Bolsdorfer (+21.1 ± 4.0%), Hühnerberg (+18.8 ± 6.0%) and lime (+20.8 ± 6.8%) base saturation increased significantly at day 135 and subsequently declined (Figure 3; Table S7).

With the exception of pore water Al and Na, treatment did not significantly affect pore water elemental or nutrient concentrations (Figure S8-S10). Hühnerberg significantly reduced pore water Al compared to control (-0.17 ± 0.07 mg l^{-1}; Figure S8), whereas Bolsdorfer and Eifelgold treatments significantly increased pore water Na compared to control (+5.94 ± 2.29 and +4.41 ± 2.31 mg l^{-1} for Bolsdorfer and Eifelgold respectively; values are mean ± SE; Figure S9; Table S7).

Crop biomass and quality

Maize biomass density generally varied significantly between growing seasons, with very little treatment effects (Figure 5; Table S6). Corn, leaf and root biomass significantly decreased between the first and the second growing season, whereas stem biomass did not differ significantly between growing seasons. A significant treatment x growing season interaction effect emerged on stem biomass; however, a post-hoc comparison revealed only a trend for an

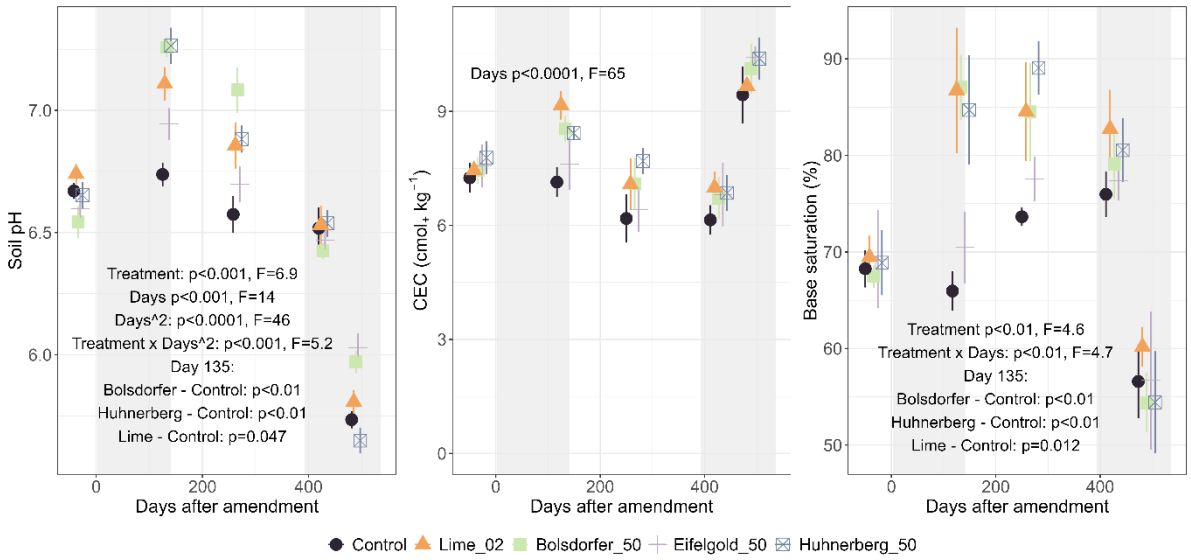


***Figure 3**: Average soil pH (left), potential cation exchange capacity (CEC, middle) and base saturation (right) throughout the experiment for each treatment. Error bars represent the standard error on the mean. Shadowed areas represent the growing seasons. Significant p- and F-values are shown from a linear mixed model with soil pH, CEC or base saturation as response variable, days as continuous covariate, treatment as class covariate and plot as random effect. Significant pairwise comparisons from post-hoc tests are indicated. Significant interaction effects, when present, are indicated in the plot by an "x". When interactions were not significant, they were excluded from the model and not shown here. See Table S7 for complete statistics.*

increase in stem biomass with Hühnerberg at the end of the second growing season (p=0.056; +0.53 ± 0.16 kg m^{-2}; mean ± SE). Treatment did not affect total aboveground biomass (Figure S11).

Treatment effects on maize nutrient concentrations were generally absent, with two exceptions (Figures S12-S16; Table S6). First, root C content significantly decreased with lime (-5.99 ±3.1 %) and Eifelgold (-8.82 ± 0.82 %) compared to control at the end of the first growing season (values are mean ± SE; Figure S14). Second, Hühnerberg significantly increased root Mg compared to control (+0.140 ±0.024 mg g^{-1}; average increase across two growing season ± SE; Figure S16). Despite significant treatment x growing season interaction effects on corn and leaf BSi, the post-hoc tests did not reveal any significant treatment effect within each growing season (Figure S12). None of the treatments significantly affected C:N ratio, N, Ni or Cr content in any of the plant parts.

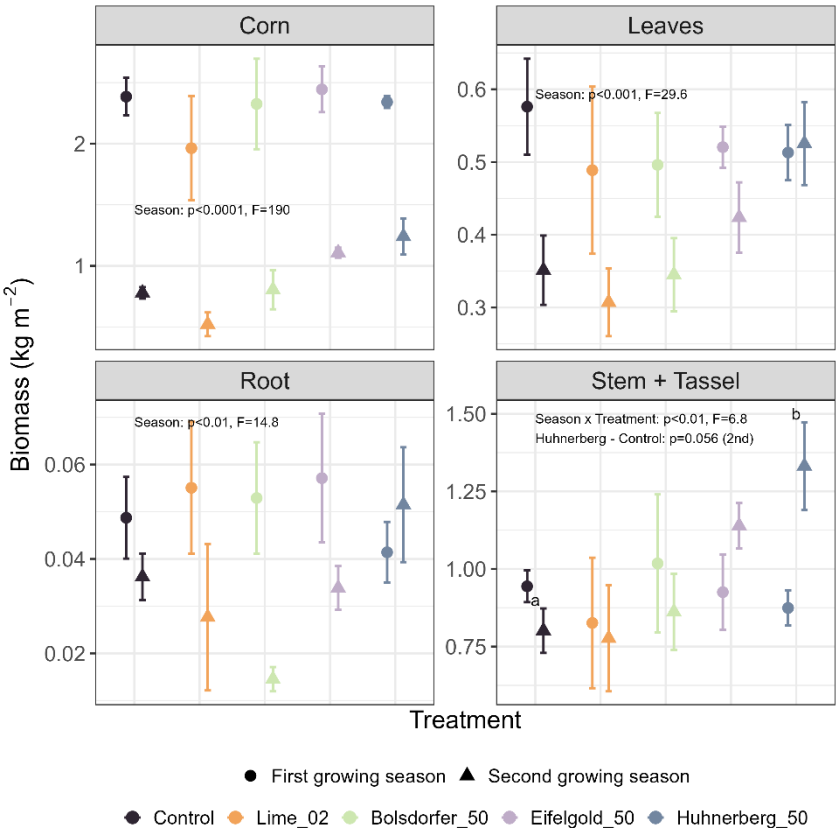


***Figure 5**: Average biomass density for each organ, for each treatment and for each growing season. Error bars represent the standard error on the mean. Significant p- and F- values are shown from a factorial analysis of variance (ANOVA) performed with biomass as response variable, treatment and growing season as fixed effects and plot as a random effect. Significant pairwise comparisons from post-hoc tests are indicated. Significant interaction effects, when present, are indicated in the plot by an "x". When interactions were not significant, they were excluded from the model and not shown here. See Table S6 for complete statistics.*

Discussion

Weathering signals: pore water pH, alkalinity and DIC

Overall, our data reveal consistent weathering signals across most feedstocks, reflected in increases in pore water DIC and alkalinity, with the notable exception of Eifelgold tephrite, for which these increases were not statistically significant. Across all silicates, weathering indicators were strongest during the early stages of the experiment and declined over time, though they did not disappear entirely. This suggests that weathering persisted beyond the first growing season, albeit possibly at reduced rates. The comparable effects of Bolsdorfer and Hühnerberg basalts and lime on pore water DIC (and partially alkalinity, for which the increase with lime had $p=0.07$) further suggest that these basalts sustained comparatively high initial weathering rates.

As silicates weather, they consume protons and release cations, leading to the formation of dissolved (bi)carbonate (Hartmann et al., 2013). This process elevates soil pH as well as pore water alkalinity and DIC. The observed patterns are therefore consistent with expectations and with previous findings (Amann and Hartmann, 2022; Amann et al., 2020; Beerling et al., 2024; Steinwidder et al., 2025). Nevertheless, the detection of a weathering signal under field conditions cannot be assumed. At the field-scale, soil processes can dilute or even obscure treatment effects, as illustrated by Dupla et al. (2025), who reported minimal impacts of silicate additions on weathering proxies such as pore water DIC and pH. There, the authors attributed the absence of a detectable signal to slow mineral dissolution kinetics combined with high soil heterogeneity, which possibly influenced EW responses and their detection in our field experiment as well.

Effect of silicate mineralogy and lime

We hypothesized that silicates containing faster-weathering minerals, such as Bolsdorfer basalt, would exert stronger effects on soil properties and crop performance, while lime would produce more immediate but short-lived effects due to its rapid dissolution. In particular, Bolsdorfer basalt contained three times more nepheline (which weathers more than 300 and 200 times faster than diopside and labradorite, an intermediate plagioclase feldspar, respectively, under neutral mechanism at 25 °C; Palandri and Kharaka, 2004) than Eifelgold tephrite, while Hühnerberg did not contain any nepheline (Table 2). In addition, Bolsdorfer basalt contained twice as much diopside than Hühnerberg basalt, a pyroxene with intermediate weathering rates (Gudbrandsson et al., 2011).

Overall, our data shows that soil responses cannot simply be predicted from mineralogy: while Bolsdorfer basalt produced pronounced early responses, as it significantly increased pore water alkalinity, DIC, Na, soil pH and base saturation, a similar response was observed for Hühnerberg basalt, which also significantly increased pore water pH, DIC, alkalinity, soil pH and base saturation, despite being composed of relatively slower-weathering minerals compared to Bolsdorfer. Hühnerberg contained substantially higher amounts of plagioclase relative to Bolsdorfer basalt (0 vs. 26.5%), which likely contributed to proton consumption and base-cation release during weathering. However, plagioclase dissolution rates vary strongly based on their anorthite content (Palandri and Kharaka, 2004), therefore plagioclase's contribution to the feedstock's weathering rates cannot be exactly quantified. In addition, small differences in particle size distribution and specific surface area among the basalts (which strongly influence reactive mineral surface availability and therefore mineral dissolution rates) may also have

contributed to the variability observed among treatments. Te Pas et al. (2023) and Buckingham and Henderson (2024) also observed distinct pH and alkalinity responses of different basalt feedstocks in soil column experiments. However, results of Buckingham and Henderson (2024) showed that basalt increased pore water pH, an effect only observed with Hühnerberg basalt in our field experiment, thus highlighting the challenges of translating laboratory findings to field settings.

Concerning plant and soil responses, lime did not outperform the silicates, thus contradicting our hypothesis of a stronger but shorter lime effect compared to silicates, owing to lime's faster dissolution rates (Palandri and Kharaka, 2004). Instead, the effects of lime closely mirrored those of Bolsdorfer and Hühnerberg basalts, apart from an increase in pore water Na with Bolsdorfer (absent in lime due to its lack of Na; Figure S9). Notably, the above-mentioned soil column experiment by Buckingham and Henderson (2024) also found that basalt-induced increases in pore water alkalinity were comparable to those generated by lime, an outcome that aligns with our findings.

Soil water content

Our results only partially support the hypothesis that feedstock amendments would increase soil VWC. Significant increases in VWC were observed only following Hühnerberg and Eifelgold application, and these effects were restricted to the first growing season. In contrast, during the fallow period, Hühnerberg, Bolsdorfer and lime significantly decreased VWC, whereas no treatment effects were detected during the second growing season.

Taken together, our VWC results suggest that amendment effects may be governed by the balance between an immediate physical change following amendment incorporation and slower changes in soil structure associated with weathering, which develop over time. Shortly after application, feedstock particles may occupy existing pore spaces and shift the pore size distribution towards smaller pores. Such changes could increase water retention as water is held more strongly within finer pores (Hillel, 1998). This mechanism may occur immediately following incorporation, before substantial weathering has taken place, owing to the physical presence of amendment particles within the soil matrix. The transient increase in VWC observed for Hühnerberg and Eifelgold during the first growing season is consistent with this interpretation and with results from Akortey et al. (2026), who found an increase in water retention after glacial rock flour addition, and attributed it to the amendment filling pore spaces. A recent review effort by Gholamahmadi et al. (2026) showed that silicate amendments increased soil moisture by a median of +4.4%, thus agreeing with our results during the first growing season. However, because this effect was not consistently observed across all feedstocks and did not persist over time, particle-induced pore filling alone is unlikely to fully explain the observed treatment responses.

Additional processes may have contributed to the lower VWC observed with lime, Bolsdorfer and Hühnerberg during the fallow period. Compared with silicate amendments, in our field experiment lime was applied at a much lower rate (2 vs. 50 ton ha^{-1}). Therefore, given the lower amount of particles added in the lime treatment, the physical effect might be insignificant here. On the other hand, the faster dissolution rates of lime compared to silicates was likely associated with higher Ca release (Palandri and Kharaka, 2004), which may have facilitated the formation of stable macroaggregates through cation bridging and cementation (Blume et al., 2010; Bronick and Lal, 2005), thereby increasing the proportion of inter-aggregate pore space (Carmeis Filho et al., 2016; Ferreira et al., 2019; Hamza et al., 2026). These structural changes could facilitate pore

connectivity, water flow and drainage (Mangalassery et al., 2013; Uchida et al., 2008), thus reducing VWC. While aggregate formation and water flow pathways were not assessed in the present study, this mechanism could provide a potential explanation for the responses observed for lime.

On one hand, plant water uptake and transpiration, together with evaporation, also likely influenced overall soil moisture dynamics, as shown by the generally higher VWC recorded during the fallow period compared to the growing seasons. On the other hand, plant transpiration alone is unlikely to account for the treatment-specific responses observed in this study. During the first growing season, the higher VWC observed following Eifelgold and Hühnerberg application could theoretically reflect reduced transpiration. However, this explanation appears unlikely to account for a substantial proportion of the observed response, as none of the treatments significantly affected aboveground biomass, which would generally be expected to differ if plant water use varied markedly among treatments. Further evidence against a dominant role of transpiration emerges from the fallow period data, during which effects on VWC persisted. Following harvest, vegetation cover and associated transpiration were strongly reduced, while lower temperatures also limited atmospheric evaporative demand. Under these conditions, treatment-induced differences in VWC are unlikely to have been driven primarily by changes in evapotranspiration. Nevertheless, as evapotranspiration was not measured directly, its contribution to the growing-season responses cannot be fully quantified.

In addition to variation in evapotranspiration, treatment-induced changes in soil structural properties likely contributed to the temporal dynamics of VWC. Specifically, the temporal patterns observed throughout the experiment suggest that the dominant processes controlling VWC may shift over time. Whereas physical pore-filling may initially increase water retention, this effect might diminish as feedstock particles weather and soil structure evolves, and weathering-induced changes in soil aggregation and pore connectivity may become increasingly important. Under such a scenario, an initial increase in VWC could weaken or even reverse over time, depending on the balance between water retention, percolation and evapotranspiration processes. The observed increase of VWC with Hühnerberg during the first growing season, followed by a significant VWC decrease with the same treatment during the fallow period are consistent with this conceptual framework, although direct evidence for these processes was not collected. Still, our results are supported by results from a mesocosm experiment by Boito et al. (2025), in which basalt addition to mesocosms planted with maize increased soil water content during the first growing season, while it decreased it during the fallow period and second growing season.

Interestingly, the decline in VWC with Bolsdorfer basalt was only observed between day 284 and 304. This delayed response may be related to differences in mineralogy and weathering products. The relatively rapid weathering of Bolsdorfer basalt is largely attributable to its nepheline content (Table 2), a Na-rich mineral that releases primarily the monovalent cation Na^+ (and in smaller measure K^+) upon dissolution (Manning, 2010). In contrast to Ca^{2+} and Mg^{2+}, Na^+ does not generally contribute to cation bridging and can even reduce the degree of flocculation (Blume et al., 2010). Consequently, the initial stages of Bolsdorfer weathering would not be expected to enhance soil structure. As weathering progressed, however, the slower dissolution of Ca- and Mg-bearing minerals may have increased the supply of polyvalent cations capable of promoting aggregate formation. Such a delayed structural response could explain why VWC in Bolsdorfer treatment remained similar to the control during most of the fallow period, but began to decline towards the end of it, when weathering of these minerals may have become more prominent.

Unfortunately, interpretation of the observed temporal trends is complicated by field management practices. Harvesting operations conducted between the first growing season and the subsequent fallow period likely affected soil physical conditions through machinery traffic, while ploughing between the fallow period and the second growing season likely disrupted soil aggregates and altered pore connectivity (Blume et al., 2010; Bronick and Lal, 2005). Indeed, VWC was very similar across treatments during the second growing season. Consequently, our study design did not allow assessment of how amendment-induced structural changes would evolve under undisturbed conditions. It therefore remains uncertain whether the observed responses would have persisted, disappeared or shifted over longer time scales. Further work involving direct measurements of aggregation, pore-size distribution, water flow and retention would be required to test the mechanisms proposed here.

Soil chemical fertility and nutrient availability

The characteristics of the starting soil (pH = 6.6, SOC = 2.7 %) indicate that soil chemical fertility was already high prior to amendment, which likely constrained the potential for additional soil and crop improvements. Within such contexts, EW might therefore prove more relevant as a CDR strategy rather than a means of delivering agronomic co-benefits, especially since crop performance also showed no improvement (see below). Our hypothesis that rock amendments would improve soil chemical fertility (i.e., soil pH, CEC and base saturation) is therefore only partially supported, as the only significant changes observed were short-lived: increases in soil pH and base saturation with Hühnerberg, Bolsdorfer and lime disappeared after the first growing season.

In addition, while increases in pH and CEC are commonly reported outcomes of enhanced weathering (Anda et al., 2015; Conceição et al., 2022; Gillman, 1980; Rijnders et al., 2023; Rijnders et al., 2025; Skov et al., 2024; Ten Berge et al., 2012; Xu et al., 2025), we found no statistically significant increase in CEC following amendment application. Interestingly, CEC increased over time in the control plots, a trend primarily driven by the higher CEC values observed during the last sampling event (day 491, on 23 September 2024). This overall temporal increase may be attributable to field management practices, particularly manure applications (Blume et al., 2010). Despite the observed temporal increase, the CEC values observed in this experiment (8.6 ± 0.2 $cmol^+ kg^{-1}$; mean ± SE) fall within the expected range for Podzols (~11 $cmol^+ kg^{-1}$) (White, 2005), and are at the lower end for soils of similar texture but slightly lower SOM (10–25 cmol+ kg^{-1} for sandy loams, loams, and silt loams with 2–3% SOM and illite, smectite, and vermiculite clays)(Blume et al., 2010).

Crop biomass and quality

Contrary to our initial hypothesis and consistent with our soil data, crop biomass and quality were driven primarily by seasonal variability rather than by the applied amendments. Across both growing seasons, basalt, tephrite, and lime failed to produce consistent changes in maize biomass or quality, and the few treatment-specific differences that arose were neither systematic (i.e., consistent across various plant organs) nor repeated across growing seasons. Overall, under the relatively fertile starting conditions of this field trial, the geochemical shifts induced by EW did not translate into measurable agronomic benefits.

Such limited crop responses align with findings from similar studies carried out in temperate regions, where EW often shows little effect on yields unless soils are strongly acidic or nutrient-depleted (Swoboda et al., 2022). Mesocosm experiments have likewise reported no significant

biomass increases with basalt application, including for potato (Vienne et al., 2022) and maize (Boito et al., 2025). However, positive responses have been documented elsewhere, for example in spring oat (Skov et al., 2024), sorghum (Kelland et al., 2020), and maize (Rijnders et al., 2025), indicating that EW's agronomic benefits can occur under specific environmental and/or edaphic conditions.

A likely explanation for these contrasting outcomes is the dependence of EW's performance on baseline soil properties. Yield improvements are most frequently reported for highly weathered, nutrient-poor soils amended with mafic or ultramafic rocks, where EW can alleviate nutrient limitations and acidity (Swoboda et al., 2022). In contrast, our experimental soil was relatively fertile, which may have limited the scope for additional nutrient supply to translate into measurable crop responses. Thus, in productive agricultural systems, EW may function primarily as a CDR strategy rather than a crop enhancement practice.

Conclusion

In this 16-month field experiment in Belgium, we tested whether three different silicate amendments with contrasting mineralogy, compared to lime, could increase soil volumetric water content (VWC), as well as enhance soil chemical fertility and crop yield and quality. We hypothesized that the amended silicates would deliver more persistent benefits than lime, with faster-weathering silicates exerting quicker effects. Increases in weathering signals (pore water dissolved inorganic carbon (DIC) and alkalinity) indicated that weathering was active in our experiment, especially during the first growing season after amendment.

Despite sustained weathering, treatment effects on soil chemical fertility (pH, cation exchange capacity and base saturation) were overall limited and largely short-lived, and they did not translate into effects on crop biomass and quality. Hühnerberg basalt and Eifelgold tephrite significantly increased VWC during the first growing season, whereas Hühnerberg, Bolsdorfer and lime significantly reduced VWC during the subsequent fallow period. These findings suggest that silicate amendments can influence soil hydrological properties, but that such effects might be dependent on amendment mineralogy and time since application. Overall, our results indicate that, in agricultural systems using relatively fertile soil such as the one used in this experiment, the primary value of EW may lie in its CO_2 removal potential rather than in consistent agronomic gains.

Conflict of interests

The authors declare no conflicts of interest.

Funding

This work was supported by the Research Foundation – Flanders (FWO) through Ph.D. Fellowships awarded to A.V. (Grant No. 1S06325N), L.S. (Grant No. 1174925N), and C.V. (Grant No. 11T4225N). T.N. is currently supported by the University of Antwerp Special Research Fund (BOF; Grant No. FN542400002). This research also received support from the C-Farms (Grant No. S004023N) and the UPSURGE projects (Grant No. 101003818).

Acknowledgments

We thank Mintjens BV, and especially Karel Mintjens and Wim de Cordt, for their openness in dedicating one of their fields to this experiment and for their continued logistical support. We gratefully acknowledge the contributions of Inge Van de Putte, for her support in establishing the experiment. We also thank the numerous (job)students whose assistance with establishment and data collection was invaluable to this work.

Data availability

The data and model code in support of our findings are openly available in Zenodo at https://doi.org/10.5281/zenodo.23803780 (Boito, 2026). All figures, tables, and textual content presented in this manuscript were created by the authors. No third-party copyrighted material has been reproduced; therefore, no permissions for reuse were required.

References

Akortey, W., Oppong Danso, E., Dietzen, C., Amponsah, W., Arthur, E., Boadi Mensah, B. K., Obour, P. B., Nyasapoh, J. B. A., Darko, D. A., Dorvlo, S. Y., Sabi, E. B., Abenney-Mickson, S., and Rosing, M. T.: Short-term effects of Greenlandic glacial rock flour on soil physical properties and maize yield, Nutrient Cycling in Agroecosystems, 132, 10.1007/s10705-025-10452-2, 2026.

Amann, T. and Hartmann, J.: Ideas and perspectives: Synergies from co-deployment of negative emission technologies, Biogeosciences, 16, 2949–2960, 10.5194/bg-16-2949-2019, 2019.

Amann, T. and Hartmann, J.: Carbon Accounting for Enhanced Weathering, Frontiers in Climate, 4, 10.3389/fclim.2022.849948, 2022.

Amann, T., Hartmann, J., Struyf, E., de Oliveira Garcia, W., Fischer, E. K., Janssens, I., Meire, P., and Schoelynck, J.: Enhanced Weathering and related element fluxes – a cropland mesocosm approach, Biogeosciences, 17, 103–119, 10.5194/bg-17-103-2020, 2020.

Anda, M., Shamshuddin, J., and Fauziah, C. I.: Improving chemical properties of a highly weathered soil using finely ground basalt rocks, Catena, 124, 147–161, 10.1016/j.catena.2014.09.012, 2015.

Araujo, F. S. M., Chacon, A. G. M., Porto, R. F., Cavalcante, J. P. L., Chiang, Y. W., and Santos, R. M.: Adapting and Verifying the Liming Index for Enhanced Rock Weathering Minerals as an Alternative Liming Approach, Land, 13, 10.3390/land13111839, 2024.

Basta, N., Pantone, D., and Tabatabai, M.: Path analysis of heavy metal adsorption by soil, Agronomy Journal, 85, 1054–1057, https://doi.org/10.2134/agronj1993.00021962008500050018x, 1993.

Beerling, D. J., Leake, J. R., Long, S. P., Scholes, J. D., Ton, J., Nelson, P. N., Bird, M., Kantzas, E., Taylor, L. L., Sarkar, B., Kelland, M., DeLucia, E., Kantola, I., Muller, C., Rau, G., and Hansen, J.: Farming with crops and rocks to address global climate, food and soil security, Nat Plants, 4, 138–147, 10.1038/s41477-018-0108-y, 2018.

Beerling, D. J., Epihov, D. Z., Kantola, I. B., Masters, M. D., Reershemius, T., Planavsky, N. J., Reinhard, C. T., Jordan, J. S., Thorne, S. J., Weber, J., Val Martin, M., Freckleton, R. P., Hartley, S. E., James, R. H., Pearce, C. R., DeLucia, E. H., and Banwart, S. A.: Enhanced weathering in the US Corn Belt delivers carbon removal with agronomic benefits, Proc Natl Acad Sci U S A, 121, e2319436121, 10.1073/pnas.2319436121, 2024.

Beerling, D. J., Kantzas, E. P., Lomas, M. R., Wade, P., Eufrasio, R. M., Renforth, P., Sarkar, B., Andrews, M. G., James, R. H., Pearce, C. R., Mercure, J. F., Pollitt, H., Holden, P. B., Edwards, N. R., Khanna, M., Koh, L., Quegan, S., Pidgeon, N. F., Janssens, I. A., Hansen, J., and Banwart, S. A.:

584 Potential for large-scale CO(2) removal via enhanced rock weathering with croplands, Nature,
585 583, 242–248, 10.1038/s41586-020-2448-9, 2020.
586 Blume, H. P., Brümmer, G. W., Horn, R., Kandeler, E., Kögel-Knabner, I., Kretzschmar, R., Stahr, K.,
587 Wilke, B.-M., Thiele-Bruhn, S., and Welp, G.: Scheffer/schachtschabel, Lehrbuch der
588 Bodenkunde, 472, 10–1007 pp., 978-3-642-30942-7, 10.1007/978-3-642-30942-7, 2010.
589 Boito, L., Steinwidder, L., Rijnders, J., Berwouts, J., Janse, S., Niron, H., Roussard, J., Vienne, A.,
590 and Vicca, S.: Enhanced Rock Weathering Altered Soil Organic Carbon Fluxes in a Plant Trial, Glob
591 Chang Biol, 31, e70373, 10.1111/gcb.70373, 2025.
592 Boito, L. N., T.; Vandenhove, C.; Van Ryckeghem, L.; Steinwidder, L.; Vienne, A.; Janssens, I.;
593 Vicca, S. : Soil and crop responses to basalt, tephrite and lime amendments in a 16-month maize
594 field trial (1), Zenodo [dataset], https://doi.org/10.5281/zenodo.23803780, 2026.
595 Bronick, C. J. and Lal, R.: Soil structure and management: a review, Geoderma, 124, 3–22,
596 https://doi.org/10.1016/j.geoderma.2004.03.005, 2005.
597 Buckingham, F. L. and Henderson, G. M.: The enhanced weathering potential of a range of silicate
598 and carbonate additions in a UK agricultural soil, Sci Total Environ, 907, 167701,
599 10.1016/j.scitotenv.2023.167701, 2024.
600 Carmeis Filho, A. C., Crusciol, C. A., Guimaraes, T. M., Calonego, J. C., and Mooney, S. J.: Impact
601 of Amendments on the Physical Properties of Soil under Tropical Long-Term No Till Conditions,
602 PLoS One, 11, e0167564, 10.1371/journal.pone.0167564, 2016.
603 Clarkson, M. O., Larkin, C. S., Swoboda, P., Reershemius, T., Suhrhoff, T. J., Maesano, C. N., and
604 Campbell, J. S.: A review of measurement for quantification of carbon dioxide removal by
605 enhanced weathering in soil, Frontiers in Climate, 6, 10.3389/fclim.2024.1345224, 2024.
606 Conceição, L. T., Silva, G. N., Holsback, H. M. S., Oliveira, C. d. F., Marcante, N. C., Martins, É. d.
607 S., Santos, F. L. d. S., and Santos, E. F.: Potential of basalt dust to improve soil fertility and crop
608 nutrition, Journal of Agriculture and Food Research, 10, 10.1016/j.jafr.2022.100443, 2022.
609 de Oliveira Garcia, W., Amann, T., Hartmann, J., Karstens, K., Popp, A., Boysen, L. R., Smith, P.,
610 and Goll, D.: Impacts of enhanced weathering on biomass production for negative emission
611 technologies and soil hydrology, Biogeosciences, 17, 2107–2133, 10.5194/bg-17-2107-2020,
612 2020.
613 DeMaster, D. J.: The supply and accumulation of silica in the marine environment, Geochimica et
614 Cosmochimica acta, 45, 1715–1732, https://doi.org/10.1016/0016-7037(81)90006-5, 1981.
615 Dietzen, C., Harrison, R., and Michelsen-Correa, S.: Effectiveness of enhanced mineral
616 weathering as a carbon sequestration tool and alternative to agricultural lime: An incubation
617 experiment, International Journal of Greenhouse Gas Control, 74, 251–258,
618 10.1016/j.ijggc.2018.05.007, 2018.
619 Dinno, A.: _dunn.test: Dunn'sTest of Multiple Comparisons Using Rank Sums_ (R package version
620 1.3.6) [code], https://CRAN.R-project.org/package=dunn.test 2024, accessed
621 Dondeyne, S., Vanierschot, L., Langohr, R., Van Ranst, E., and Deckers, J.: The soil map of the
622 Flemish region converted to the 3rd edition of the World Reference Base for soil resources, 2014.
623 Dupla, X., Bertagni, M. B., and Grand, S.: Three Years of Field Trials Indicate a Sustained Enhanced
624 Rock Weathering Signal with Limited CO(2) Removal, Environ Sci Technol, 59, 25751–25764,
625 10.1021/acs.est.5c09820, 2025.
626 Dupla, X., Möller, B., Baveye, P. C., and Grand, S.: Potential accumulation of toxic trace elements
627 in soils during enhanced rock weathering, European Journal of Soil Science, 74,
628 10.1111/ejss.13343, 2023.
629 ESRI: ArcGIS Desktop: Release 10, Environmental Systems Research Institute. [code], 2011,
630 accessed
631 Ferreira, T. R., Pires, L. F., Wildenschild, D., Brinatti, A. M., Borges, J. A. R., Auler, A. C., and dos
632 Reis, A. M. H.: Lime application effects on soil aggregate properties: Use of the mean weight
633 diameter and synchrotron-based X-ray μCT techniques, Geoderma, 338, 585–596,
634 10.1016/j.geoderma.2018.10.035, 2019.

Fuss, S., Lamb, W. F., Callaghan, M. W., Hilaire, J., Creutzig, F., Amann, T., Beringer, T., de Oliveira Garcia, W., Hartmann, J., Khanna, T., Luderer, G., Nemet, G. F., Rogelj, J., Smith, P., Vicente, J. L. V., Wilcox, J., del Mar Zamora Dominguez, M., and Minx, J. C.: Negative emissions—Part 2: Costs, potentials and side effects, Environmental Research Letters, 13, 10.1088/1748-9326/aabf9f, 2018.

Garcia-Leon, D., Casanueva, A., Standardi, G., Burgstall, A., Flouris, A. D., and Nybo, L.: Current and projected regional economic impacts of heatwaves in Europe, Nat Commun, 12, 5807, 10.1038/s41467-021-26050-z, 2021.

Gholamahmadi, B., Boito, L., Steinwidder, L., and Vicca, S.: Impacts of enhanced rock weathering on soil sponge function: a global synthesis of soil physical and hydrological responses 2, CDRXIV, 2026.

Gillman, G.: The effect of crushed basalt scoria on the cation exchange properties of a highly weathered soil, Soil Science Society of America Journal, 44, 465–468, https://doi.org/10.2136/sssaj1980.03615995004400030005x, 1980.

Gislason, S. R. and Oelkers, E. H.: Carbon storage in basalt, Science, 344, 373–374, 10.1126/science.1250828, 2014.

Goll, D. S., Ciais, P., Amann, T., Buermann, W., Chang, J., Eker, S., Hartmann, J., Janssens, I., Li, W., Obersteiner, M., Penuelas, J., Tanaka, K., and Vicca, S.: Potential CO2 removal from enhanced weathering by ecosystem responses to powdered rock, Nature Geoscience, 14, 545–549, 10.1038/s41561-021-00798-x, 2021.

Gudbrandsson, S., Wolff-Boenisch, D., Gislason, S. R., and Oelkers, E. H.: An experimental study of crystalline basalt dissolution from 2 ⩽ pH ⩽ 11 and temperatures from 5 to 75 °C, Geochimica et Cosmochimica Acta, 75, 5496–5509, 10.1016/j.gca.2011.06.035, 2011.

Habibullah, M. S., Din, B. H., Tan, S. H., and Zahid, H.: Impact of climate change on biodiversity loss: global evidence, Environ Sci Pollut Res Int, 29, 1073–1086, 10.1007/s11356-021-15702-8, 2022.

Hamza, A., Karcauskiene, D., Mockeviciene, I., Repsiene, R., Noor Us, S., and Slepetiene, A.: Re-acidification of limed soil alters aggregate stability and soil carbon turnover in an agroecosystem, RSC Adv, 16, 32730–32743, 10.1039/d6ra01955b, 2026.

Hartmann, J., West, A. J., Renforth, P., Köhler, P., De La Rocha, C. L., Wolf-Gladrow, D. A., Dürr, H. H., and Scheffran, J.: Enhanced chemical weathering as a geoengineering strategy to reduce atmospheric carbon dioxide, supply nutrients, and mitigate ocean acidification, Reviews of Geophysics, 51, 113–149, 10.1002/rog.20004, 2013.

Hillel, D.: Environmental Soil Physics, Academic Press, 1998.

IPCC: Climate Change 2022: Mitigation of Climate Change. Working Group III Contribution to the Sixth Assessment Report of the Intergovernmental Panel on Climate Change, Cambridge, UK and New York, USA, 10.1017/9781009157926, 2022,

Kabata-Pendias, A.: Trace elements in soils and plants, CRC press, 042919112X, 2000.

Kelland, M. E., Wade, P. W., Lewis, A. L., Taylor, L. L., Sarkar, B., Andrews, M. G., Lomas, M. R., Cotton, T. E. A., Kemp, S. J., James, R. H., Pearce, C. R., Hartley, S. E., Hodson, M. E., Leake, J. R., Banwart, S. A., and Beerling, D. J.: Increased yield and CO(2) sequestration potential with the C(4) cereal Sorghum bicolor cultivated in basaltic rock dust-amended agricultural soil, Glob Chang Biol, 26, 3658–3676, 10.1111/gcb.15089, 2020.

Koninklijk Meteorologisch Instituut van België: Climate atlas: https://www.meteo.be/nl/klimaat/klimaat-van-belgie/klimaatatlas/klimaatkaarten/luchttemperatuur/gemiddelde/jaarlijks, last access: 29/10/2026.

Kopecky, M., Macek, M., and Wild, J.: Topographic Wetness Index calculation guidelines based on measured soil moisture and plant species composition, Sci Total Environ, 757, 143785, 10.1016/j.scitotenv.2020.143785, 2021.

Kottek, M., Grieser, J., Beck, C., Rudolf, B., and Rubel, F.: World map of the Köppen-Geiger climate classification updated, https://doi.org/10.1127/0941-2948/2006/0130, 2006.
Kuznetsova, A., Brockhoff, P. B., and Christensen, R. H.: lmerTest package: tests in linear mixed effects models, Journal of statistical software, 82, 1–26, 10.18637/jss.v082.i13, 2017.
Lenth, R. P., J.: emmeans: Estimated Marginal Means, aka Least-Squares Means (R package version 2.0.4) [code], https://CRAN.R-project.org/package=emmeans 2026, accessed
Levy, C. R., Almaraz, M., Beerling, D. J., Raymond, P., Reinhard, C. T., Suhrhoff, T. J., and Taylor, L.: Enhanced Rock Weathering for Carbon Removal-Monitoring and Mitigating Potential Environmental Impacts on Agricultural Land, Environ Sci Technol, 58, 17215–17226, 10.1021/acs.est.4c02368, 2024.
Loomis, R. and Morris, J.: Agricultural Productivity, American Institute of Biological Sciences Circulation, AIBS, 1313 Dolley ..., 1525-3244, 1983.
Mangalassery, S., Sjögersten, S., Sparkes, D. L., Sturrock, C. J., and Mooney, S. J.: The effect of soil aggregate size on pore structure and its consequence on emission of greenhouse gases, Soil and Tillage Research, 132, 39–46, 10.1016/j.still.2013.05.003, 2013.
Manning, D. A. C.: Mineral sources of potassium for plant nutrition. A review, Agronomy for Sustainable Development, 30, 281–294, 10.1051/agro/2009023, 2010.
Palandri, J. L. and Kharaka, Y. K.: A compilation of rate parameters of water-mineral interaction kinetics for application to geochemical modeling, U.S. Department of the Interior and U.S. Geological Survey2331-1258, 70, https://doi.org/10.3133/ofr20041068, 2004,
Pinheiro, J., Bates, D., DebRoy, S., Sarkar, D., and Team, R. C.: Linear and nonlinear mixed effects models [code], https://cran.r-project.org/web/packages/nlme/nlme.pdf 2007, accessed 19/10/2026.
R Core Team: RStudio: Integrated Development Environment for R (2024.4.2.764), Posit Software PBC [code], https://dailies.rstudio.com/version/2024.04.2+764.pro1/ 2024, accessed 19/10/2026.
Renforth, P.: The potential of enhanced weathering in the UK, International Journal of Greenhouse Gas Control, 10, 229–243, 10.1016/j.ijggc.2012.06.011, 2012.
Righi, D. and Meunier, A.: Origin of Clays by Rock Weathering and Soil Formation, in: Origin and Mineralogy of Clays, Springer-Verlag, Berlin, https://doi.org/10.1007/978-3-662-12648-6_3, 1995.
Rijnders, J.: Assessing the role of enhanced weathering in sustainable agriculture: Benefits and risks for crop growth in a temperate climate, Bioscience Engineering, Universiteit Antwerpen, Antwerp, 2025.
Rijnders, J., Vienne, A., and Vicca, S.: Effects of basalt, concrete fines, and steel slag on maize growth and toxic trace element accumulation in an enhanced weathering experiment, Biogeosciences, 22, 2803–2829, 10.5194/bg-22-2803-2025, 2025.
Rijnders, J., Vicca, S., Struyf, E., Amann, T., Hartmann, J., Meire, P., Janssens, I., and Schoelynck, J.: The effects of dunite fertilization on growth and elemental composition of barley and wheat differ with dunite grain size and rainfall regimes, Frontiers in Environmental Science, 11, 10.3389/fenvs.2023.1172621, 2023.
Saccone, L., Conley, D., Koning, E., Sauer, D., Sommer, M., Kaczorek, D., Blecker, S., and Kelly, E.: Assessing the extraction and quantification of amorphous silica in soils of forest and grassland ecosystems, European Journal of Soil Science, 58, 1446–1459, https://doi.org/10.1111/j.1365-2389.2007.00949.x, 2007.
Schuiling, R. D. and Krijgsman, P.: Enhanced Weathering: An Effective and Cheap Tool to Sequester Co2, Climatic Change, 74, 349–354, 10.1007/s10584-005-3485-y, 2006.
Shamshuddin, J., Anda, M., Fauziah, C., and Omar, S. S.: Growth of cocoa planted on highly weathered soil as affected by application of basalt and/or compost, Communications in soil science and plant analysis, 42, 2751–2766, https://doi.org/10.1080/00103624.2011.622822, 2011.

Skov, K., Wardman, J., Healey, M., McBride, A., Bierowiec, T., Cooper, J., Edeh, I., George, D., Kelland, M. E., Mann, J., Manning, D., Murphy, M. J., Pape, R., Teh, Y. A., Turner, W., Wade, P., and Liu, X.: Initial agronomic benefits of enhanced weathering using basalt: A study of spring oat in a temperate climate, PLoS One, 19, e0295031, 10.1371/journal.pone.0295031, 2024.
Steinwidder, L., Boito, L., Frings, P. J., Niron, H., Rijnders, J., de Schutter, A., Vienne, A., and Vicca, S.: Beyond Inorganic C: Soil Organic C as a Key Pathway for Carbon Sequestration in Enhanced Weathering, Glob Chang Biol, 31, e70340, 10.1111/gcb.70340, 2025.
Suhrhoff, T. J.: Phytoprevention of Heavy Metal Contamination From Terrestrial Enhanced Weathering: Can Plants Save the Day?, Frontiers in Climate, 3, 10.3389/fclim.2021.820204, 2022.
Suhrhoff, T. J., Reershemius, T., Wang, J., Jordan, J. S., Reinhard, C. T., and Planavsky, N. J.: A tool for assessing the sensitivity of soil-based approaches for quantifying enhanced weathering: a US case study, Frontiers in Climate, 6, 10.3389/fclim.2024.1346117, 2024.
Swoboda, P., Doring, T. F., and Hamer, M.: Remineralizing soils? The agricultural usage of silicate rock powders: A review, Sci Total Environ, 807, 150976, 10.1016/j.scitotenv.2021.150976, 2022.
te Pas, E. E. E. M., Hagens, M., and Comans, R. N. J.: Assessment of the enhanced weathering potential of different silicate minerals to improve soil quality and sequester CO2, Frontiers in Climate, 4, 10.3389/fclim.2022.954064, 2023.
ten Berge, H. F., van der Meer, H. G., Steenhuizen, J. W., Goedhart, P. W., Knops, P., and Verhagen, J.: Olivine weathering in soil, and its effects on growth and nutrient uptake in Ryegrass (Lolium perenne L.): a pot experiment, PLoS One, 7, e42098, 10.1371/journal.pone.0042098, 2012.
Uchida, Y., Clough, T., Kelliher, F., and Sherlock, R.: Effects of aggregate size, soil compaction, and bovine urine on N2O emissions from a pasture soil, Soil Biology and Biochemistry, 40, 924–931, 10.1016/j.soilbio.2007.11.007, 2008.
Vaghetti Luchese, A., Pivetta, L. A., Batista, M. A., Steiner, F., Giaretta, A. d. S., and Curtis, J. C. D.: Agronomic feasibility of using basalt powder as soil nutrient remineralizer, Afr. J. Agric. Res, 17, 487–497, 10.5897/AJAR2020.15234 2021.
van Straaten, P.: Rocks for Crops: Agrominerals of sub-Saharan Africa, ICRAF, Nairobi, Kenya, 0-88955-512-5, 2002.
Vienne, A., Poblador, S., Portillo-Estrada, M., Hartmann, J., Ijiehon, S., Wade, P., and Vicca, S.: Enhanced Weathering Using Basalt Rock Powder: Carbon Sequestration, Co-benefits and Risks in a Mesocosm Study With Solanum tuberosum, Frontiers in Climate, 4, 10.3389/fclim.2022.869456, 2022.
White, R. E.: Principles and practice of soil science: the soil as a natural resource, John Wiley & Sons, 0632064552, 2005.
Xu, T., Li, H., Vicca, S., Goll, D. S., Beerling, D. J., Chen, Q., Bi, B., Yang, Z., Wang, X., and Yuan, Z.: Enhanced Rock Weathering Promotes Soil Organic Carbon Accumulation: A Global Meta-Analysis Based on Experimental Evidence, Glob Chang Biol, 31, e70483, 10.1111/gcb.70483, 2025.

Supplementary information related to manuscript titled "Soil and crop responses to basalt, tephrite and lime amendments in a 16-month maize field trial"

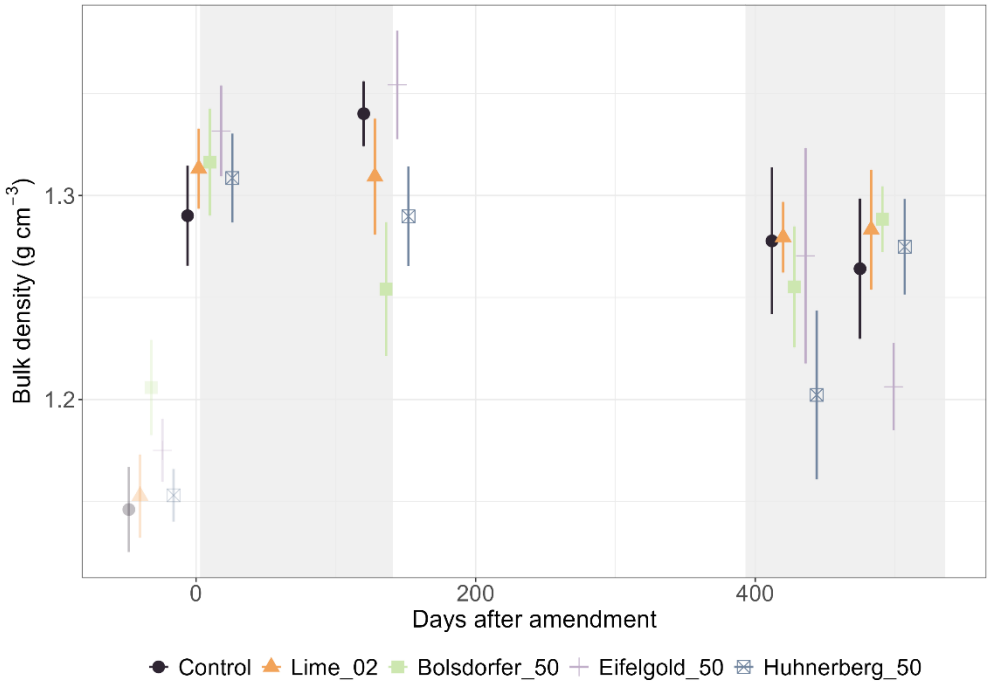


***Figure S1**: Average bulk density for each treatment throughout the experiment. Shaded grey areas represent the growing seasons. Error bars represent the standard error on the mean.*

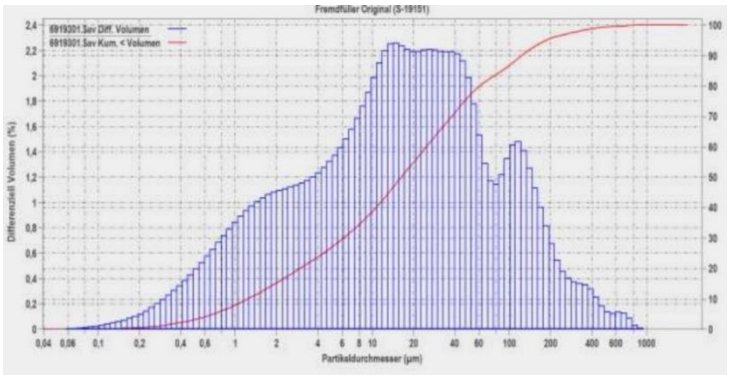


***Figure S2**: Particle size distribution (d80 = 62.3 µm) of Hühnerberg basalt. Provided by RPBL.*

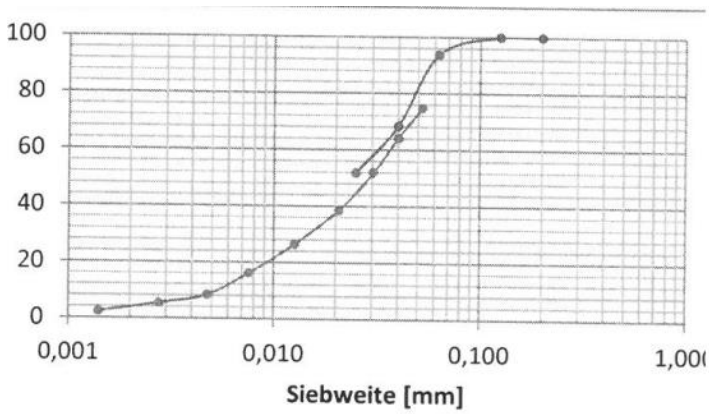


***Figure S3**: Particle size distribution (d80 = 84.4 µm) of Eifelgold tephrite. Provided by RPBL.*

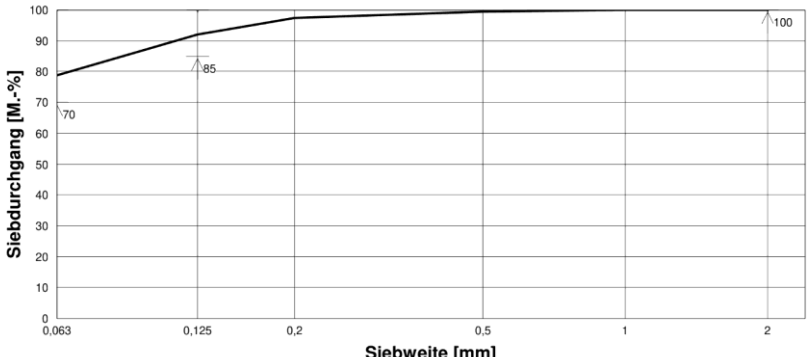


***Figure S4**: Particle size distribution (d80 = 78.4 µm) of Bolsdorfer basalt. Provided by RPBL.*



***Figure S5**: Example of the area (delimited by yellow measuring tape) randomly selected in each plot for above- and below-ground biomass sampling.*

***Table S6**: p- and F- (or chi²) values for analyses on plant data (ANOVA), with treatment, growing season and their interaction (if significant) as explanatory variables. When assumptions of normality and homoscedasticity were not met, a non-parametric test (Kruskal-Wallis, indicated in brackets) was performed. Significance of pairwise comparisons (estimated with post-hoc tests) is also indicated. Treatment names are C = control, L = lime, BD = Bolsdorfer, EG = Eifelgold, HBG = Hühnerberg. Significant effects (p<0.05) are indicated in **bold**, while trends (0.05<p<0.09) are indicated in italics. Continues on next page.*

Response variable	Unit	Treatment	Growing season	Treatment x Growing season
Total aboveground biomass	Kg m^{-2}	P=0.38, F=1.2	**P<0.0001, F=60.4**	n.s.
Corn biomass	Kg m^{-2}	P=0.24, F=1.65	**P<0.0001, F=190.0**	n.s.
Leaf biomass	Kg m^{-2}	P=0.59, F=0.73	**P<0.001, F=29.63**	*P=0.072, F=3.01*
Root biomass	Kg m^{-2}	P=0.86, F=0.32	**P<0.01, F=14.76**	*P=0.074, F=2.98*
Stem + Tassel biomass	Kg m^{-2}	P=0.5, F=0.9	P=0.19, F=2.02	**P<0.01, F=6.8** **HBG – C: p=0.056 (2nd)**
Corn BSi	Log10 (mg g^{-1})	P=0.41, F=1.1	**P<0.0001, F=218.7**	**P=0.012, F=3.47**
Leaf BSi	Log10 (mg g^{-1})	P=0.79, F=0.41	**P<0.0001, F=63.44**	**P=0.014, F=3.36**
Root BSi	mg g^{-1}	P=0.48, F=0.5	**P<0.0001, F=115.77**	n.s.
Stem BSi	mg g^{-1}	P=0.14, F=2.23	**P<0.0001, F=833.0**	n.s.
Corn C	%	P=0.22, F=1.48	P=0.48, F=0.49	n.s.
Leaf C	%	P=0.17, chi^2 = 6.4 (Kruskal-Wallis)	**P<0.0001, chi^2 = 40.49 (Kruskal-Wallis)**	n.s.
Root C	%	*P=0.057, F=2.81*	**P<0.0001, F=71.22**	*P=0.057, F=2.81* *EG – C: p<0.01 (1st)* *L – C: p=0.033 (1st)*
Stem C	%	P=0.45, F=1.0	**P<0.0001, F=326.3**	n.s.
Corn N	%	P=0.25, F=1.59	**P<0.001, F=15.54**	n.s.
Leaf N	%	P=0.94, F=0.2	**P<0.0001, F=441.4**	n.s.
Root N	%	P=0.4, F=1.12	**P<0.001, F=22.03**	n.s.
Stem N	%	P=0.23, F=1.69	**P<0.0001, F=23.1**	n.s.
Corn C:N	g g^{-1}	P=0.35, F=1.24	**P<0.0001, F=19.7**	n.s.
Leaf C:N	g g^{-1}	P = 0.94, chi^2 = 0.81 (Kruskal-Wallis)	**P<0.0001, chi^2 = 64.28 (Kruskal-Wallis)**	n.s.
Root C:N	g g^{-1}	P=0.56, F=0.79	**P=0.01, F=9.15**	n.s.
Stem C:N	g g^{-1}	P=0.4, F=1.12	**P<0.0001, F=39.15**	n.s.
Corn Ca	Ln (mg g^{-1})	P=0.37, F=1.19	**P<0.0001, F=118.34**	n.s.
Leaf Ca	ln(mg g^{-1})	P=0.41, chi^2 = 4.01 (Kruskal-Wallis)	**P<0.0001, chi^2 = 33.95 (Kruskal-Wallis)**	n.s.

785

***Table S6**: continued.*

Response variable	Unit	Treatment	Growing season	Treatment x Growing season
Root Ca	ln(mg g^{-1})	P=0.78, F=0.44	P=0.54, F=0.4	n.s.
Stem Ca	ln(mg g^{-1})	P=0.34, chi^2 = 4.49 (Kruskal-Wallis)	**P<0.0001, chi^2 = 27.73(Kruskal-Wallis)**	n.s.
Corn Fe	mg g^{-1}	**P=0.022, F=4.72** *L – C: p=0.102*	**P<0.0001, F=105.5**	n.s.
Leaf Fe	ln(mg g^{-1})	*P=0.093, chi^2 = 0.82* (Kruskal-Wallis)	**P<0.0001, chi^2 = 63.75 (Kruskal-Wallis)**	n.s.
Root Fe	Log10 (mg g^{-1})	P=0.89, F=0.26	**P<0.0001, F=124.2**	n.s.
Stem Fe	Log10 (mg g^{-1})	P=0.82, F=0.38	**P<0.0001, F=85.5**	n.s.
Corn Mg	Log10 (mg g^{-1})	P=0.46, F=0.99	P=0.15, F=2.08	n.s.
Leaf Mg	Log10 (mg g^{-1})	P=0.54, chi^2 = 3.13 (Kruskal-Wallis)	**P<0.0001, chi^2 = 55.9 (Kruskal-Wallis)**	n.s.
Root Mg	√(mg g^{-1})	**P<0.01, F=5.45** **HBG – C: p=0.02**	**P=0.018, F=6.83**	n.s.
Stem Mg	Log10 (mg g^{-1})	P=0.14, F=2.24	**P<0.0001, F=26.54**	n.s.
Corn K	Log10 (mg g^{-1})	P=0.52, F=0.86	**P<0.0001, F=872.6**	n.s.
Leaf K	Log10 (mg g^{-1})	P=0.88, F=0.28	**P<0.0001, F=64.17**	n.s.
Root K	Log10 (mg g^{-1})	P=0.61, F=0.71	*P=0.075, F=4.19*	n.s.
Stem K	Log10 (mg g^{-1})	P=0.22, F=1.47	**P<0.0001, F=77.59**	n.s.
Corn P	Log10 (mg g^{-1})	P=0.52, F=0.86	**P<0.0001, F=338.75**	n.s.
Leaf P	Log10 (mg g^{-1})	P=0.99, chi^2 = 0.18 (Kruskal-Wallis)	**P<0.0001, chi^2 = 60.14 (Kruskal-Wallis)**	n.s.
Root P	√ (mg g^{-1})	P=0.88, F=0.28	**P<0.001, F=25.12**	n.s.
Stem P	Log10 (mg g^{-1})	P=0.35, F=1.25	**P<0.0001, F=306.93**	n.s.
Corn Cr	Log10 (mg g^{-1})	p=0.42, chi^2 =3.91 (Kruskal-Wallis)	**P<0.01, chi^2 = 10.46 (Kruskal-Wallis)**	n.s.
Leaf Cr	Log10 (mg g^{-1})	P=0.95, chi^2 = 0.69 (Kruskal-Wallis)	**P<0.0001, chi^2 = 65.23 (Kruskal-Wallis)**	n.s.
Root Cr	mg g^{-1}	P=0.65, chi^2 = 2.49 (Kruskal-Wallis)	**P<0.0001, chi^2 = 16.2 (Kruskal-Wallis)**	n.s.
Stem Cr	mg g^{-1}	P=0.87, F=0.31	**P<0.0001, F=160.9**	n.s.
Leaf Ni	Log10 (mg g^{-1})	P=0.83, F=0.37	**P<0.0001, F=373.42**	n.s.
Root Ni	√ (mg g^{-1})	P=0.37, F=1.19	**P=0.035, F=5.97**	n.s.
Stem Ni	Log10 (mg g^{-1})	P=0.86, F=0.32	**P<0.0001, F=116.61**	n.s.

***Table S7**: p- and F- values from linear mixed models built to test for effects on pore water data, volumetric water content (VWC), soil pH, CEC and base saturation. Days (continuous covariate), treatment (class covariate), and their interaction (if significant) were used as explanatory variables. Significant post-hoc comparisons between treatment and controls are indicated. **Bold** indicates significant effects (p<0.05), while italic symbolizes trends (0.05 < p < 0.09). Treatment names are C = control, L = lime, BD = bolsdorfer, EG = Eifelgold, HBG = Huhnerberg. Continues on next page.*

Response variable	Unit	Treatment	Days	Days x Treatment
Pore water pH	unitless	**P=0.019, F=3.06**	P=0.48, F=0.5	n.s.
		HBG – C: p=0.038		
Pore water DIC	Log10(mg L^{-1} +1)	**P<0.0001, F=7.97**	**P<0.001, F=13.83**	n.s.
		BD – C: p=0.017		
		HBG – C: p<0.01		
		L – C: p<0.01		
Pore water alkalinity	√ (meq L^{-1})	**P<0.001, F=5.6**	**P=0.017, F=5.85**	n.s.
		BD – C: p=0.029		
		HBG – C: p=0.0112		
		L – C: p=0.0697		
Pore water DOC	Log10(mg L^{-1})	P=0.86, F=0.33	**P<0.0001, F=23.83**	n.s.
Pore water Al	√ (mg L^{-1})	**P=0.01, F=3.44**	P=0.87, F=0.03	n.s.
		HBG – C: p=0.03		
Pore water Ca	Log10(mg L^{-1})	P=0.34, F=1.28	**P<0.0001, F=32.1**	n.s.
Pore water Mg	Log10(mg L^{-1})	P=0.14, F=1.77	**P<0.0001, F=43.3**	n.s.
Pore water K	Log10(mg L^{-1})	P=0.49, F=0.86	**P<0.0001, F=16.2**	
Pore water Fe	Log10(mg L^{-1})	P=0.93, F=0.2	P=0.59, F=0.29	n.s.
Pore water Na	Log10(mg L^{-1})	**P<0.01, F=9.63**	**P<0.0001, F=36.46**	n.s.
		BD – C: p<0.01		
		EG – C:p=0.019		
Pore water NO_3^--N	Log10(mg L^{-1})	P=0.88, F=0.3	**P<0.01, F=7.06**	n.s.
Pore water NH_4^+-N	√ (mg L^{-1})	P=0.38, F=1.07	**P<0.0001, F=28.7**	n.s.
Pore water Ni	mg L^{-1}	*P=0.09, F=2.06*	P=0.45, F=0.56	n.s.
Pore water PO_4^--P	√ (mg L^{-1})	P=0.95, F=0.17	**P<0.0001, F=27.3**	n.s.
Pore water SO_4	Log10(mg L^{-1})	P=0.99, F=0.04	P=0.77, F=0.08	n.s.
VWC	√%	1st: p=0.39, F=1.13	**1st: p<0.0001, F=521.9**	**1st: p<0.001, F=7.21** **EG – C: p<0.0001** **HGB – C: p<0.001**
		Winter: p=0.8, F=0.41	**Winter: p<0.0001, F=773.7**	**Winter: p<0.0001, F=14.8** **BD – C: p<0.01** **HGB – C: p<0.0001** **L – C: p<0.0001**
		2nd: p=0.98, F=0.11	**2nd: p<0.0001, F=181.3**	2nd: n.s.

***Table S7**: continued.*

Response variable	Unit	Treatment	Days	Days x Treatment
Soil pH	Unitless	**P<0.001, F=6.9**	**Days = p<0.001, F=14.0**	**Treatment x Days^2= p<0.001, F=5.2**
		BD – C: p=0.0013, 0.0053 (day 135, 265)	**Days^2 = p<0.0001, F=46**	
		HBG – C: p=0.0025, 0.02 (day 133, 265)		
		L – C: p=0.0474, *0.082* **(day 135, 265)**		
Soil CEC	Log10(cmol$_+$ kg^{-1})	P=0.36, F=1.2	**P<0.0001, F=65**	n.s.
Base saturation	%	**P=0.004, F=4.6**	**Days = p=0.29, F=1.2**	**Treatment x Day = p<0.01, F=4.7**
		BD – C: p<0.01	**Days^2 = p=0.43, F=0.7**	**BD – C: p=0.042**
		HGB – C: p<0.01		*HGB – C: p=0.063*
		L – C: p=0.012		

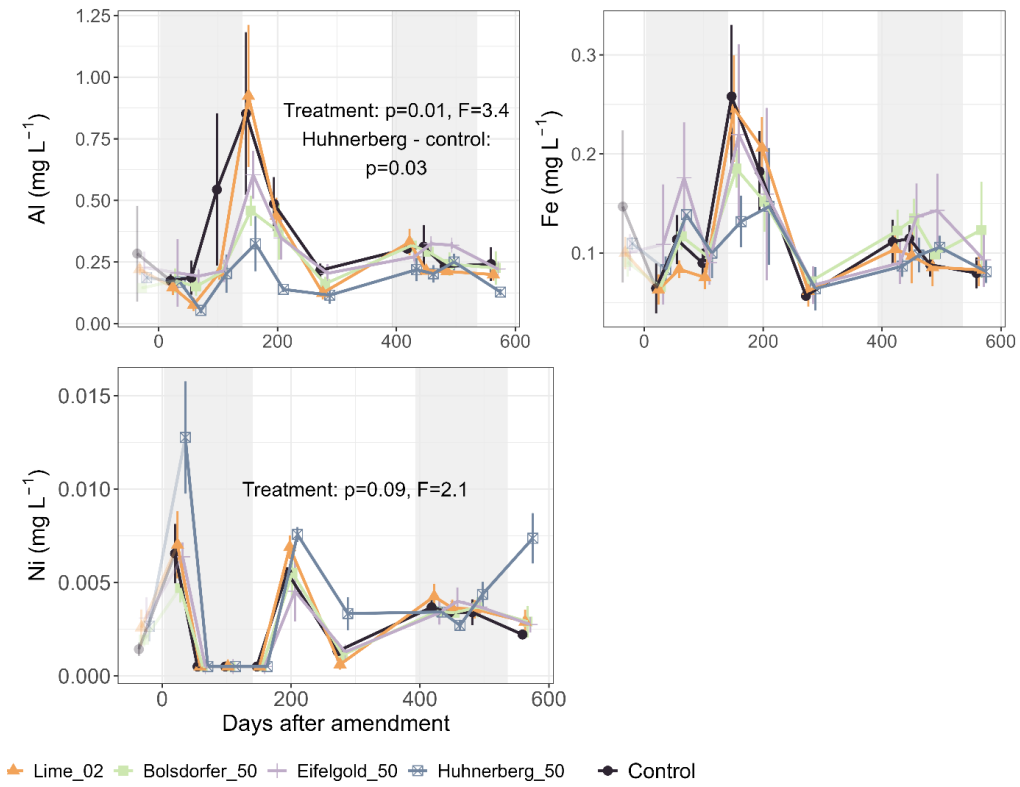


***Figure S8**: Average pore water Al, Fe, and Ni concentrations for each treatment throughout the experimental period. Error bars represent the standard error on the mean. Significant effects are presented in the plots and in Table S7. The limit of quantification (LOQ), below which the element's presence was detected, but its concentration was too low to be quantified, was 0.001 mg/l. Elemental concentration analyses were conducted in-house on samples filtered through a disposable 0.45 µm PET-45/25 membrane filter (CHROMAFIL, Macherey-Nagel) and used two quality controls measured every 25 samples prepared from Certified Reference Material (CPAChem; P/N: RM035359L25).*

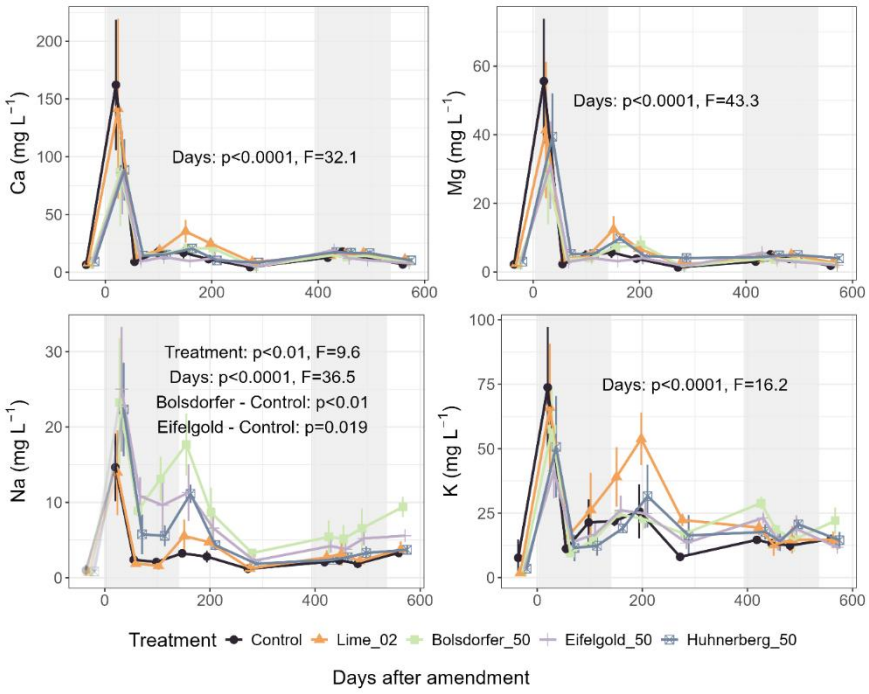


***Figure S9**: Average pore water Ca, Mg, Na and K concentrations for each treatment throughout the experimental period. Error bars represent the standard error on the mean. Significant effects are presented in the plots and in table S7. Elemental concentration analyses used two quality controls measured every 25 samples prepared from Certified Reference Material (CPAChem; P/N: RM035359L25). Analyses were conducted in-house on samples filtered through a disposable 0.45 µm PET-45/25 membrane filter (CHROMAFIL, Macherey-Nagel).*

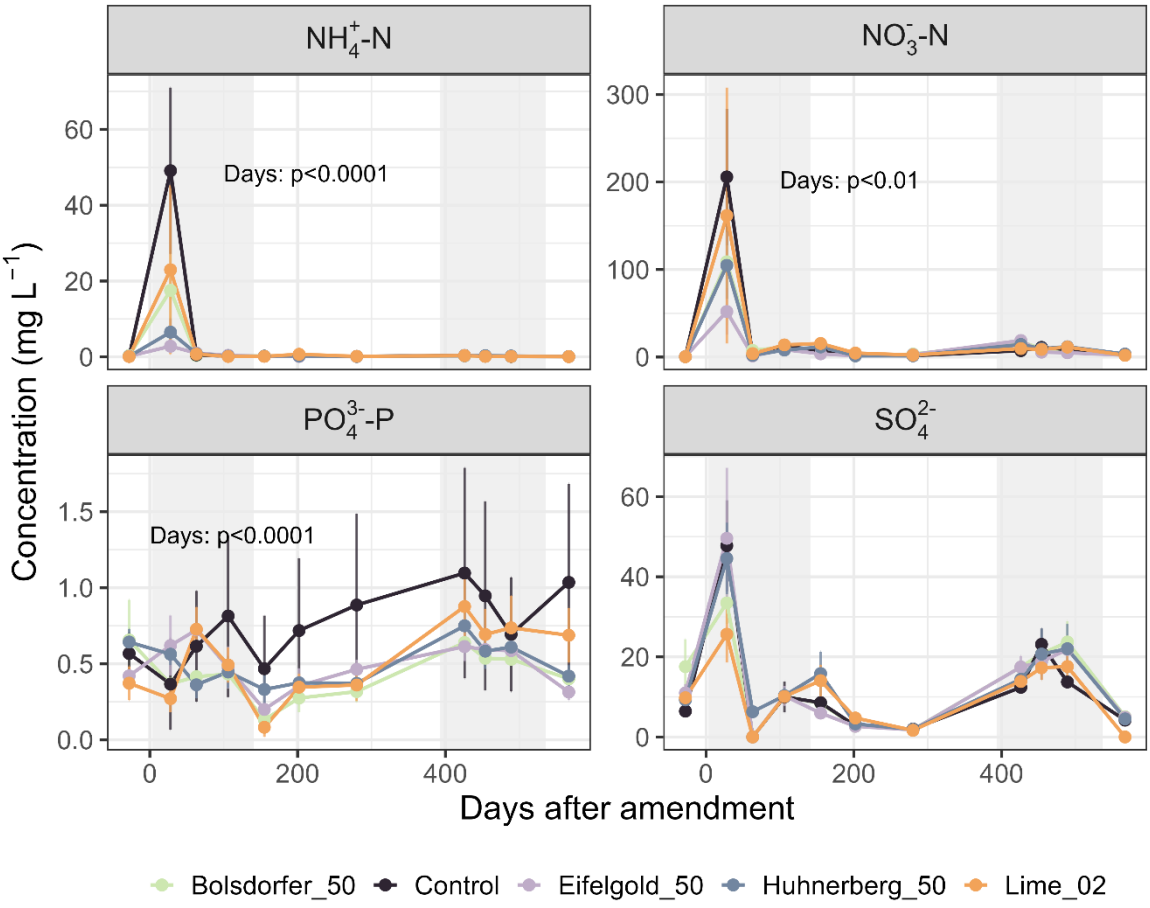


***Figure S10**: Average concentration of NH_4^+-N, NO_3^--N, PO_4^{3-}-N and SO_4^{2-} in the pore water for each treatment throughout the experiment. Error bars represent the standard error on the mean. Significant effects, when present, are indicated in the plot. The limit of quantification (LOQ), below which the element's presence was detected, but its concentration was too low to be quantified, was 0.001 mg/l. NH_4^+-N, NO_3^--N, PO_4^{3-}-P and SO_4^{2-} were measured on three technical replicates by a continuous flow analyser (SAN++® Advanced Series, Skalar) using standard NH_4^+, NO_3^-, PO_4^{3-} and SO_4^{2-} solutions (Certipur, Supelco) as quality controls respectively. NH_4^+-N, NO_3^--N, PO_4^{3-}, SO_4^{2-} analyses were conducted in-house on samples filtered through a disposable 0.45 µm PET-45/25 membrane filter (CHROMAFIL, Macherey-Nagel).*

813

814

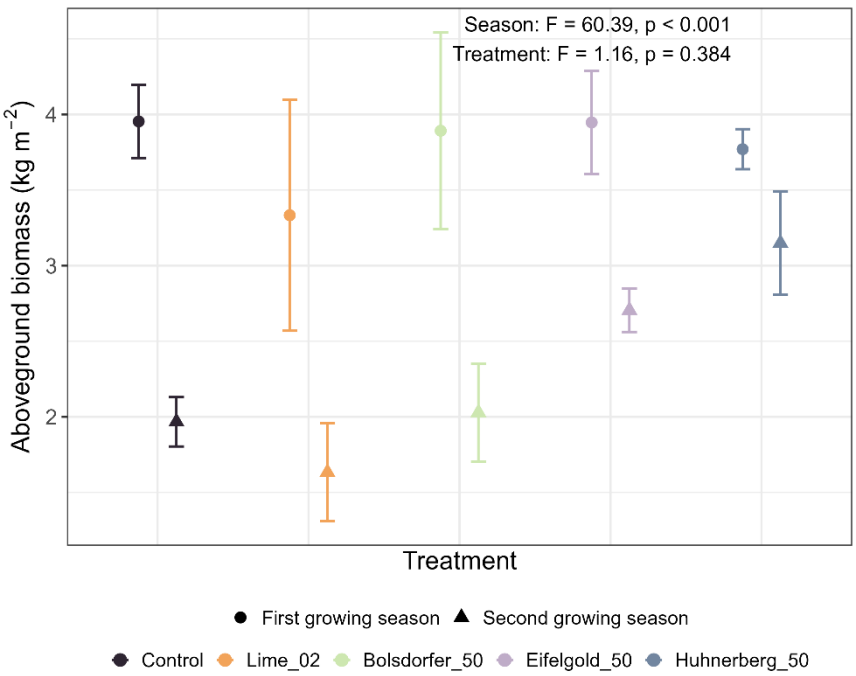


Figure S11: *Average biomass density for each treatment and growing season. Error bars represent the standard error on the mean. p- and F-values are shown from a factorial analysis of variance (ANOVA) performed with biomass as response variable, treatment and growing season as fixed effects and plot as a random effect. Significant interaction effects were tested and excluded when not significant.*

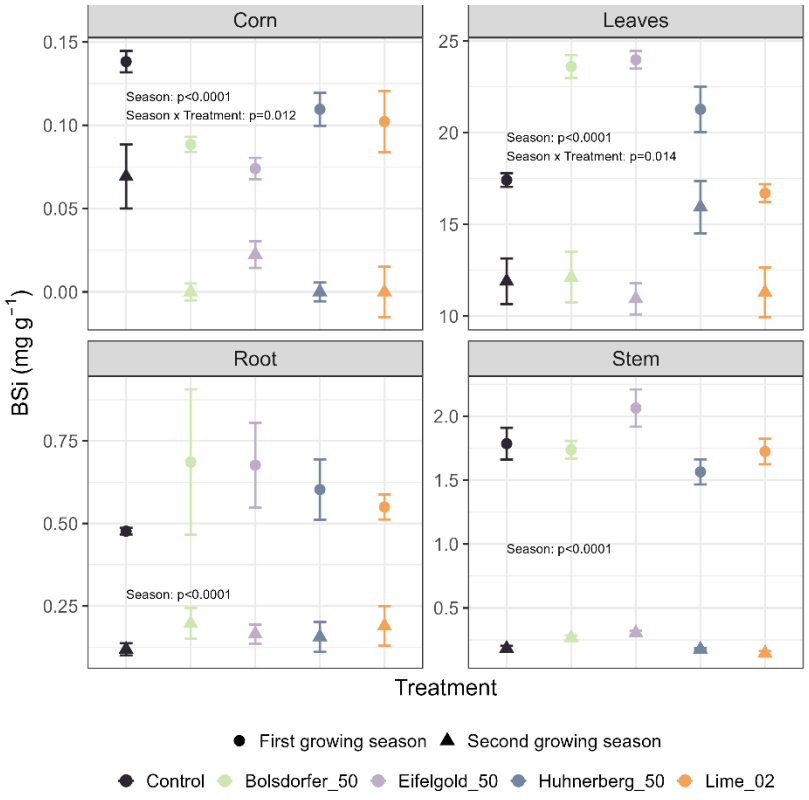


Figure S12*: Average biogenic Si (BSi) concentration in each organ, for each treatment and growing season. Error bars represent the standard error on the mean. Significant effects, when present, are indicated in the plot. See Table S6 for complete statistics.*

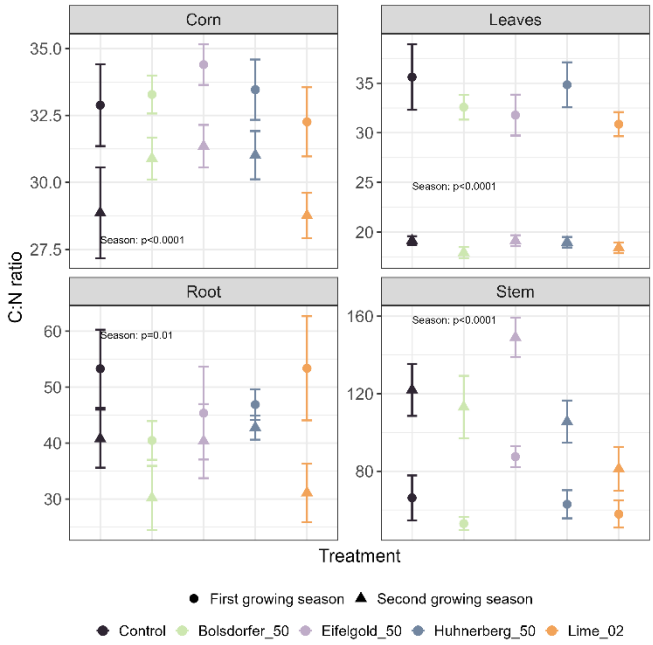


***Figure S13**: Average C:N ratio in each organ, for each treatment and growing season. Error bars represent the standard error on the mean. Significant effects, when present, are indicated in the plot. One outlier, determined by z score standardization as being > 3 SD, was removed. See Table S6 for complete statistics.*

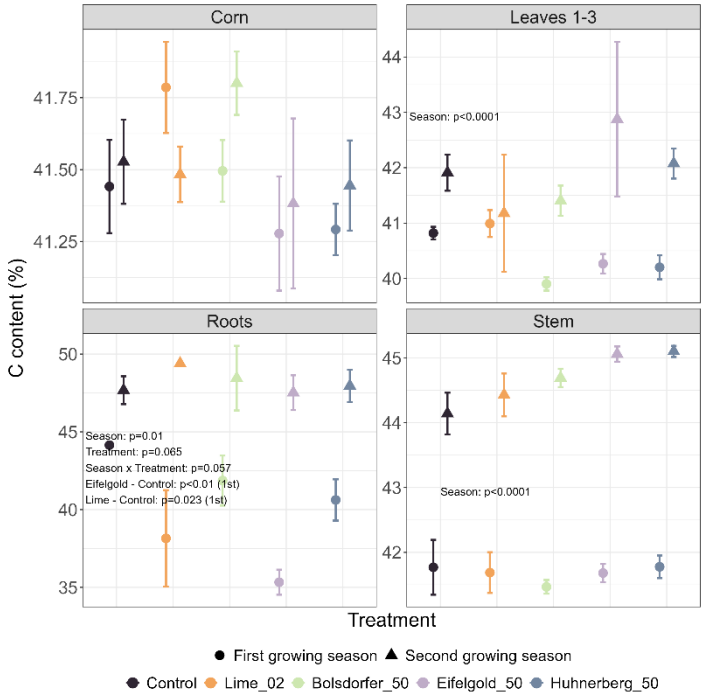


***Figure S14**: Average C content in each organ, for each treatment and growing season. Error bars represent the standard error on the mean. Significant effects, when present, are indicated in the plot. See Table S6 for complete statistics.*

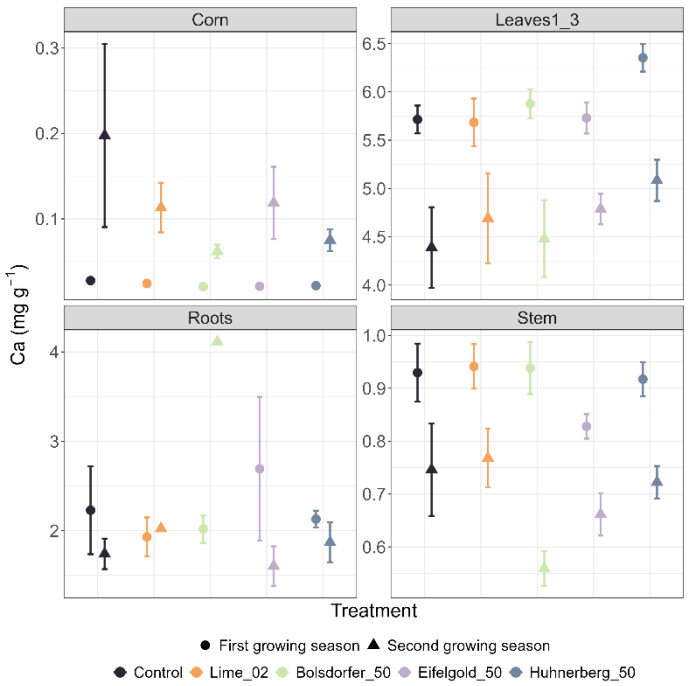


Figure S15: *Average Ca concentration in each organ, for each treatment and growing season. Error bars represent the standard error on the mean. Significant effects, when present, are indicated in the plot. Four outliers, determined by z score standardization as being > 3 SD, were removed. See Table S6 for complete statistics.*

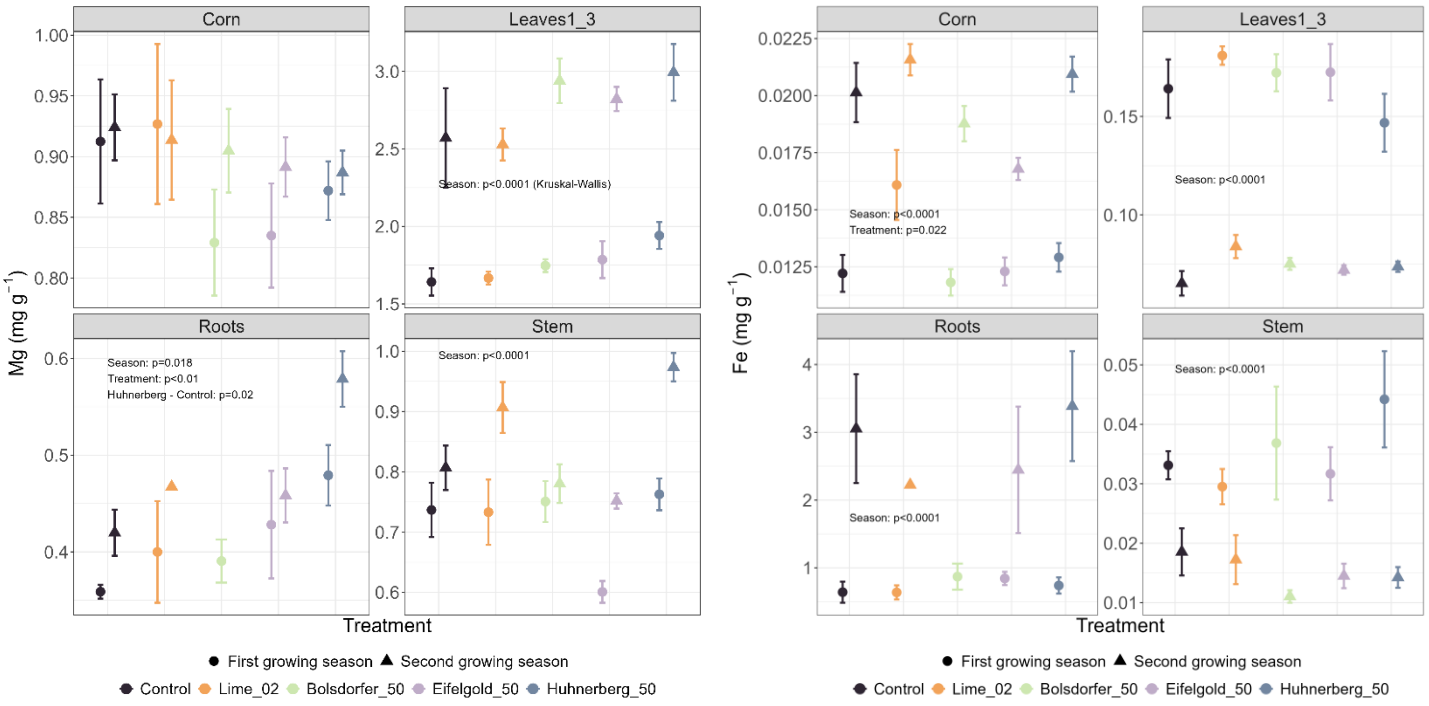


Figure S16*: Average Mg (left panel) and Fe (right panel) concentration in each organ, for each treatment and growing season. Error bars represent the standard error on the mean. Significant effects, when present, are indicated in the plot. Six (Fe) and two (Mg) outliers, determined by z score standardization as being > 3 SD, were removed. See Table S6 for complete statistics.*